# Sustainable Food Technology

Accepted Manuscript

This article can be cited before page numbers have been issued, to do this please use: B. maphosa, T. Mpanza , E. Crouch and A. A. Tsige, *Sustainable Food Technol.*, 2026, DOI: 10.1039/D6FB00142D.




ROYAL SOCIETY OF CHEMISTRY

## Sustainability Spotlight Statement

View Article Online
DOI: 10.1039/D6FB00142D

- Reduces postharvest losses in table grape supply chains through improved packaging and cold chain design.
- Enhances resource efficiency by minimizing energy use during precooling, storage, and transport.
- Addresses airflow and microclimate variability to improve consistency and reduce waste.
- Optimizes $SO_2$ application to balance decay control with reduced chemical risks and residue concerns.
- Promotes data-driven decision-making using sensors, modelling, and predictive analytics.
- Supports the development of integrated, configuration-specific cold chain systems.
- Contributes to more sustainable, resilient, and competitive fresh produce export systems.

View Article Online
DOI: 10.1039/D6FB00142D

# Packaging and cold chain optimization for quality preservation in the table grape supply chain: A Review

Buhle Maphosa[a], Thalente Mpanza[a,b], Elke Crouch[a] Alemayehu Ambaw Tsige [a,] *

[a]*Department of Horticultural Science, Packaging and Cold Chain Research Group, Africa Institute for Postharvest Technology, Faculty of AgriSciences, Stellenbosch University, Stellenbosch, South Africa*

[b]*Department of Mechanical and Mechatronic Engineering, Stellenbosch University, Private Bag X1, Matieland 7602, South Africa.*

***Corresponding author:** tsige@sun.ac.za (AA Tsige)



## Abstract

Table grapes are highly perishable and economically important commodities, requiring tightly controlled postharvest systems to maintain quality during extended export chains. This review demonstrates that quality preservation is not governed by individual factors in isolation, but by the coupled interactions between temperature, relative humidity, packaging architecture, and $SO_2$-mediated decay control. Across studies, widely adopted cold chain protocols are shown to inadequately account for the heterogeneous microenvironments created within modern multi-layer packaging systems, resulting in significant within-package and within-pallet variability that ultimately determines fruit quality outcomes. Advances in modified atmosphere and humidity-regulating packaging, dual-phase $SO_2$-generating pads, and smart liner technologies are critically evaluated in terms of their effectiveness in controlling *Botrytis cinerea* while minimizing bleaching and residue risks. Sensor-based monitoring, imaging tools, and IoT-enabled systems are examined for their capacity to quantify cold chain integrity and capture spatiotemporal variability. The review further highlights the emerging role of multiphase, multiphysics convection–diffusion–reaction modelling as a unifying framework to resolve airflow, temperature, and gas transport within packed systems. Key challenges identified include non-uniform airflow in palletized configurations, limited standardization of $SO_2$ application, and the absence of integrated, data-driven control strategies. Future progress requires a shift toward configuration-specific, mechanistically informed cold chain design supported by predictive analytics and digital twin approaches. Such advances are essential to improve storage reliability, reduce postharvest losses, and enhance the sustainability and competitiveness of the global table grape industry.

**Keywords:** Cold chain logistics; Packaging technologies; Postharvest quality preservation; $SO_2$ generator pads; Ventilation and airflow distribution; Moisture loss management; Computational Fluid Dynamics (CFD); Diffusion–reaction modelling; Temperature and humidity monitoring; Cold chain optimization.

## 1 Introduction

Table grapes (*Vitis vinifera L.*) are among the most economically important fresh fruit commodities traded globally, yet their high perishability and sensitivity to postharvest conditions

View Article Online
DOI: 10.1039/D6FB00142D





make quality preservation a persistent challenge in the cold chains. Physiological processes such as water loss, stem browning, berry softening, and susceptibility to *Botrytis cinerea* and other decay organisms intensify under non-optimum temperature and humidity conditions.[1-3] Maintaining fruit quality therefore requires a carefully coordinated system of packaging, cooling, gas management, and logistics that operate synergistically from harvest to final market. Failures at any stage of the cold chain, notably during field heat removal, forced-air precooling, refrigerated transport, or distribution, have been associated with significant losses in both berry and rachis quality, as well as economic and environmental impacts.[4, 5]

Packaging remains a critical interface between the fruit and its storage environment, governing not only protection and handling efficiency but also airflow, temperature distribution, moisture dynamics, and gas exchange around bunches. Vent hole geometry, liner perforation density, carton depth and footprint, and internal components such as clamshells or punnets directly affect airflow resistance and cooling uniformity within packed and palletized configurations.[6-9] Packaging materials in table grapes can significantly influence moisture loss, as studies have shown that internal plastic liners reduce berry transpiration but may also raise humidity levels and promote condensate formation when ventilation is inadequate.[9, 10] Evidence from other fruit cold chains, including pomegranate and citrus, further demonstrates how liner design, film permeability, and vent configuration interact with physiological water-loss pathways to determine mass loss and related disorders.[7, 11, 12] These principles have direct implications for table grapes, where moisture imbalance accelerates rachis dehydration and compromises shelf-life.

Sulphur dioxide remains the most effective and commercially dominant method for controlling *Botrytis cinerea* in table grapes during storage and shipping.[13, 14] Modern dual-phase $SO_2$ generator pads deliver an initial antimicrobial “burst” followed by sustained release to maintain suppressive concentrations. However, achieving effective $SO_2$ exposure is complicated by interactions with packaging design, liner permeability, airflow, temperature, and non-target absorption by carton materials.[15] Uneven $SO_2$ distribution due to airflow heterogeneity within cartons or across pallets may lead to overexposure in some regions, causing bleaching, and underexposure elsewhere, resulting in decay. Although $SO_2$ release and efficacy have been studied in specific cultivars and packaging systems[16, 17], comprehensive understanding of its coupled release–transport–uptake dynamics remains limited. Insights from other gas-controlled systems such as 1-MCP distribution

View Article Online
DOI: 10.1039/D6FB00142D

in apple storage[18, 19], fumigation fogging[20] , emphasize the value of mechanistic modelling in resolving spatial gas heterogeneity.

Temperature stability is a cornerstone of table grape preservation. Even short temperature increase during storage or transport can activate metabolic shifts, accelerate water loss, or diminish $SO_2$ effectiveness.[21, 22] Emerging sensor technologies, including nanosensors, MOS gas sensor, RFID-loggers, and IoT-enabled wireless networks, are increasingly used to monitor environmental parameters (temperature, humidity, atmospheric gases, spoilage markers, etc.).[23-25] Despite growing adoption, gaps remain in integrating sensor data with predictive models or control systems capable of directing operational decision-making across export supply chains.

Despite substantial progress in postharvest research, the table grape industry still lacks an integrated synthesis that connects advances in packaging design, cooling performance, $SO_2$ release technologies and airflow behaviour. Persistent challenges remain airflow and cooling often vary widely within palletized systems due to heterogeneous vent structures and stacking configurations; the mechanistic behaviour of $SO_2$, its release, movement, and absorption by berries, rachis, and packaging materials, remains insufficiently resolved under the dynamic conditions of commercial cold chains. Considering increasing demands for sustainability, traceability, and consistent quality in export markets, there is a pressing need for a comprehensive perspective that consolidates technological, physiological, and mechanistic insights into a coherent foundation for innovation. This review responds to that need by synthesizing multidisciplinary advances and identifying opportunities for data-enabled, and energy-efficient cold chain and packaging strategies for table grapes.

# 2 Packaging and cold chain management in table grapes

## 2.1 Early postharvest temperature management: shading, holding, and precooling

The postharvest cold chain of table grapes begins immediately after harvest, because physiological deterioration, water loss, and microbial development progress rapidly at ambient field temperatures. Table grapes are particularly sensitive to short delays in cooling, which can accelerate rachis browning, berry softening, and *Botrytis cinerea* development.[2, 26] Although handling practices vary across production regions, cultivars, and destinations, export-oriented

View Article Online
DOI: 10.1039/D6FB00142D

supply chains generally follow a common sequence designed to (i) rapidly remove field heat, (ii) limit dehydration, (iii) minimize mechanical injury, and (iv) deliver antifungal protection over long storage and transport durations.[17] The workflow illustrated in Figure 1 should therefore be interpreted as a representative export pathway rather than a universally standardized process.

Immediately after harvest, field shading and careful handling reduce heat gain, dehydration, and mechanical injury that can predispose clusters to rachis browning and decay.[5] In some production systems, grapes may be held briefly in shaded, evaporative, or mechanically cooled rooms prior to forced-air precooling. This holding stage is primarily a damage-limitation step (reducing heat gain and moisture loss) rather than a substitute for true precooling, and its benefit depends strongly on ambient conditions and duration.[27] Evaporative holding reduces air temperature through adiabatic cooling and typically increases relative humidity, temporarily lowering vapour pressure deficit (VPD) and thereby suppressing cluster transpiration when ambient conditions are favourable. However, its cooling potential is constrained by wet-bulb depression and is therefore climate-dependent. In contrast, mechanically cooled holding offers more climate-independent control of air temperature, but unless configured as a forced-air precooling system with appropriate airflow paths and pressure differentials, it usually cannot achieve the rate and uniformity of pulp temperature reduction required for packed export units.[28] Consequently, forced-air precooling remains the dominant “field heat removal” step in commercial export workflows .[5]

View Article Online
DOI: 10.1039/D6FB00142D



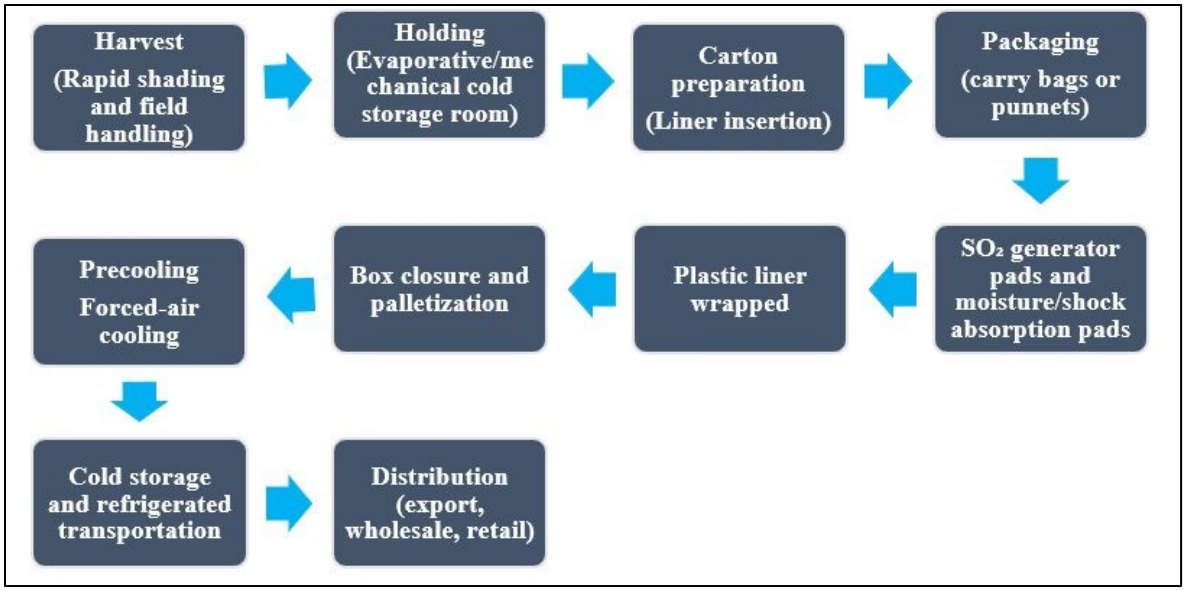


Figure 1 Schematic representation of a typical postharvest handling and cold chain workflow for export-oriented table grapes.

Figure 2 illustrates the psychrometric behaviour of early postharvest air-handling strategies for table grapes (P1–P3). The dashed trajectories depict evaporative holding, represented as near-constant-enthalpy cooling that reduces vapour-pressure deficit without requiring active dehumidification. In contrast, the solid trajectories represent mechanical air cooling, which first cools air sensibly at a constant humidity ratio and then continues along the saturation curve as condensation occurs. Together, these pathways demonstrate how early holding strategies alter the moisture–temperature relationship of the air mass before the fruit undergoes forced-air precooling.

In practice, however, these psychrometric transitions are rarely controlled explicitly in commercial operations. Early holding conditions are often governed by ambient environments or loosely managed cooling systems, resulting in limited control over vapour-pressure deficit and moisture gradients. This reflects both the documented variability in temperature–humidity conditions in

View Article Online
DOI: 10.1039/D6FB00142D

commercial cold chains and the fact that psychrometric variables, although fundamental, are often not explicitly understood or operationally managed in postharvest systemsr.[29, 30]

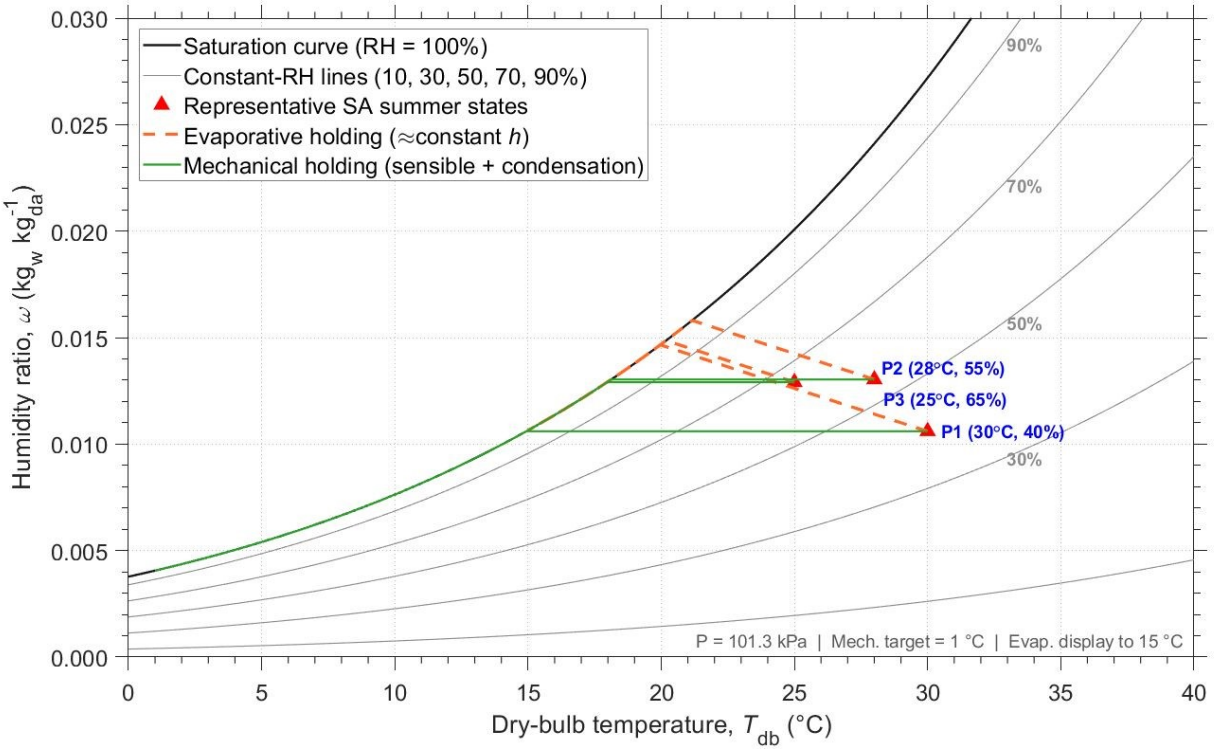


Figure 2: Psychrometric representation of early postharvest air-handling strategies for table grapes under representative South African summer conditions (P1–P3).

## 2.2 Forced-air precooling

Forced-air precooling is applied to fully packaged and palletized grapes to remove field heat under conditions that approximate subsequent cold storage and refrigerated transport. Rapid pulp temperature reduction suppresses respiration, transpiration, and fungal development. However, packaging components (liners, punnets, pads, and carton boxes) impose airflow and thermal resistances, making cooling rate and temperature uniformity strongly dependent on packaging design and pallet configuration. Cooling heterogeneity can persist into storage and transport, increasing the risk of localized decay, rachis dehydration, and uneven $SO_2$ exposure.[5, 20] Operationally, pulp temperature after packing is typically brought to –0.5 to 1 °C, a range shown to support extended storage life. For example, table grapes can be stored at –0.5 °C and 95% RH

View Article Online
DOI: 10.1039/D6FB00142D

for 40–100 days, depending on the cultivar.[9, 17] Following precooling, pallets transition into cold storage or refrigerated transport, where stable temperatures, high relative humidity, and uniform airflow remain essential to maintaining quality over long export periods.[5] Throughout this chain, fruit physiology, packaging design, cooling strategy, and $SO_2$ delivery interact dynamically, collectively determining postharvest performance and storage longevity.

Table grapes are known to be sensitive to low-temperature stress, with quality deterioration and physiological damage occurring when temperature thresholds are exceeded, particularly under prolonged exposure or uneven temperature conditions.[30,17] In this context, airflow heterogeneity within palletized systems may simultaneously generate regions of delayed cooling (hotspots) and overcooled zones (cold spots), thereby increasing the risk of freezing injury alongside other quality defects. [20] These effects highlight the importance of considering spatial temperature distribution, rather than only mean pulp temperature, in defining safe and effective precooling strategies.

Following precooling, pallets transition into cold storage or refrigerated transport, where stable temperatures, high relative humidity, and uniform airflow remain essential to maintaining quality over long export periods.[5, 20] Throughout this chain, fruit physiology, packaging design, cooling strategy, and $SO_2$ delivery interact dynamically, collectively determining postharvest performance and storage longevity.

### 2.3 Water loss pathways, rachis desiccation, and visual quality failure

Water loss is among the most consequential determinants of table grape marketability. Even at 0–1 °C and 90–95% RH, clusters continue to lose moisture via transpiration of both berries and rachis tissues.[10] Under cold storage, berry transpiration is relatively low compared with rachis transpiration, because the rachis has a porous epidermis, exposed vascular tissues, and limited cuticular protection.[2, 31] As a result, the rachis contributes disproportionately to visible deterioration that modest cumulative cluster mass losses (often only a few percent) can trigger rachis browning and shrivelling that drives consumer rejection before large changes in berry firmness or soluble solids are evident.[2, 31]

Rachis desiccation is governed by temperature and vapour pressure deficit (VPD). Temperature breaks and low-RH episodes increase VPD and accelerate rachis water loss, making cold-chain

View Article Online
DOI: 10.1039/D6FB00142D





stability a first-order quality driver.[4, 5] Even modest increases in VPD can markedly increase rachis dehydration, and visible browning can develop within days depending on cultivar and storage history.[2, 31] Experimental studies have reported reduced mass loss and less rachis browning at higher RH (e.g., ~97% vs ~93%), consistent with the expectation that decreasing VPD slows transpiration-driven deterioration.[2] Cultivar-specific physiological and structural characteristics can influence dehydration susceptibility in table grapes during storage. Berry water loss occurs primarily through transpiration across the fruit surface and is governed by vapor pressure gradients and berry surface conductance, which may vary among cultivars.[32] In addition, differences in cell wall metabolism can affect the structural stability of berry tissues during postharvest storage. For example, cultivars with higher calcium-associated pectin integrity and lower polygalacturonase activity maintain firmer tissues and exhibit greater resistance to postharvest softening.[1] Together, these findings suggest that cultivar-dependent differences in berry surface conductance and internal cell wall stability may contribute to variability in dehydration susceptibility observed among table grape cultivars during storage. Packaging also influences rachis and fruit water-loss dynamics during storage. Highly ventilated packaging can enhance cooling efficiency but may increase the vapor pressure deficit around the bunch, promoting rachis dehydration and browning. Conversely, liners or plastic films increase relative humidity within the package, thereby reducing transpiration and fruit mass loss during storage.[9, 33]

Water loss within the package microenvironment also interacts with decay control strategies. $SO_2$ generating pads rely on moisture to activate the release of $SO_2$ from metabisulfite formulations. Consequently, excessively dry conditions within the package may limit pad activation and reduce the availability of antifungal $SO_2$, thereby compromising decay control.[14]

Temperature setpoints interact with storage duration and cultivar. Some studies suggest that limited temperature relaxation may be acceptable for shorter storage durations, whereas longer storage requires stricter temperature control to limit mould and physiological deterioration.[21, 34] In parallel, alternative cooling targets (e.g., modestly higher pulp temperatures) have been explored to reduce precooling time without compromising quality, but feasibility remains cultivar- and context-dependent.[35] This interaction highlights the need to view rachis preservation not only as a dehydration problem but as a broader microclimate management challenge. In practice, effective storage therefore requires coordinated control of (i) package humidity and vapor pressure deficit,

View Article Online
DOI: 10.1039/D6FB00142D

(ii) temperature stability that influences both transpiration and fungal growth, and (iii) integrated decay suppression systems such as $SO_2$-based technologies. Taken together, the progression of rachis desiccation and visual quality failure in table grapes reflects the interaction between intrinsic cluster physiology and the storage microenvironment. Factors such as the physiological asymmetry between berries and rachis tissues, vapour pressure deficit, cumulative mass loss thresholds, atmosphere composition, packaging configuration, and cultivar-specific metabolic characteristics collectively influence the rate at which dehydration and senescence symptoms develop.[9, 31, 36, 37]. A synthesis of the principal physiological determinants governing storage behaviour and quality deterioration in table grapes is presented in Table 1.

Table 1: Physiological determinants of storage behaviour and quality deterioration in table grapes

| Factor / cultivar group | Storage condition | Dominant physiological mechanism | Quality implication | References |
|---|---|---|---|---|
| Berry vs. rachis tissues | 0–5 °C; 90–95% RH | Rachis respiration and transpiration substantially exceed berry rates | Rachis desiccation and browning often limit shelf life before berry deterioration | 2, 31 |
| Vapour pressure deficit (VPD) | Elevated VPD during storage or handling | Increased rachis transpiration due to thin epidermal tissues | Rapid visual quality decline even at small water losses | 27 |
| Cluster mass loss threshold | ~2–5% total weight loss | Visual deterioration occurs before major biochemical changes | 2–3% loss induces rachis browning; 4–5% causes berry shrivels | 4 |
| Cuticular wax composition | Cultivar dependent | Variations in cuticle thickness and wax structure affect epidermal permeability and transpiration resistance | Cultivars with thicker or less permeable cuticles show reduced water loss and delayed shrivel | 38 |
| Berry–rachis structural ratio | Rachis ≈4% of cluster mass | Small structural component controls visual appearance | Minor rachis deterioration dominates consumer perception | 31 |
| Ethylene exposure / regulation | Ethylene presence; storage above 0 °C | Ethylene accelerated rachis senescence and oxidative activity | Rapid rachis browning and wilting; 1-MCP delays senescence and maintains rachis greenness | 36, 37 |
| Atmosphere modification ($CO_2$) | Elevated $CO_2$ during cold storage | $CO_2$ modulates oxidative metabolism and antioxidant responses associated with rachis senescence | Reduced rachis browning and improved rachis quality during storage | 37 |
| Packaging / atmosphere modification | MAP, liners, high RH | Reduced VPD and transpiration through humidity buffering inside the package | Delayed rachis dehydration and extended storage life | 9, 39 |
| 'Red Globe', 'Mystery' and 'Thompson Seedless' | 0–1 °C; 90–95 % RH | Higher metabolic activity and greater sensitivity of rachis tissues to dehydration and senescence | Shorter storage potential and higher dehydration risk | 36, 40 |
| 'Red Globe' | 0–1 °C; 90–95 % RH | Intermediate metabolic activity and moderate dehydration susceptibility of rachis tissues | Shelf life commonly constrained by progressive rachis desiccation during storage | 40 |
| 'Thompson Seedless', 'Mystery', 'Cardinal' | −1–0 °C; 90–95 % RH | Lower metabolic activity and improved tolerance to senescence-related rachis deterioration | Greater storage potential when humidity and decay control are maintained | 36, 37 |

View Article Online
DOI: 10.1039/D6FB00142D

## 2.4 Corrugated fibreboard cartons

Ventilated corrugated fibreboard cartons are central to maintaining both the structural integrity and the microclimatic performance of table grape packaging systems. Beyond providing mechanical protection during handling and transport, carton design directly governs airflow pathways that control cooling rate, temperature uniformity, moisture gradients, and the distribution and retention of $SO_2$ within palletized loads.[6] Adequate ventilation is therefore a prerequisite for effective cold chain performance, with industry guidelines indicating that base and side openings should typically exceed ~3% of the carton surface area to ensure sufficient airflow through stacked pallets.[41]

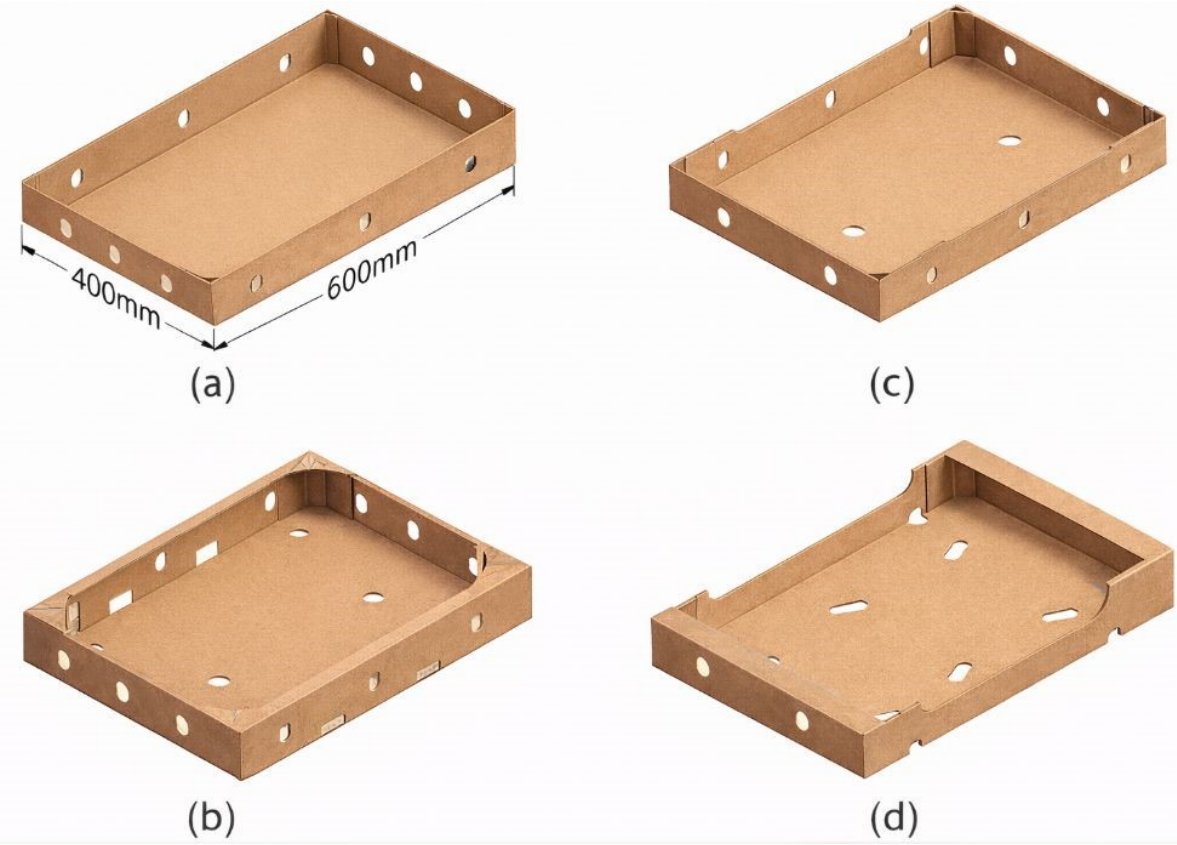


Figure 3: Ventilated corrugated fibreboard box geometries used in the table grape industry. Panel (a) shows a reference carton design with overall external dimensions (600 × 400 × 90 mm) and circular side vents, while panels (b–d) illustrate representative variations in vent-hole configuration and distribution used in commercial packaging.

View Article Online
DOI: 10.1039/D6FB00142D





The box designs illustrated in Figure 3 share a common export-standard footprint (≈600 × 400 mm), reflecting logistical constraints related to pallet modularity and forced-air precooling infrastructure. Within this standardized geometry, however, substantial variation exists in vent-hole size, shape, and spatial distribution. Boxes in Figure 3 (a) and (b) exhibit relatively balanced or moderately enhanced venting, with comparable short- and long-side openness (≈3–6%), favouring more symmetric airflow penetration and reduced sensitivity to pallet orientation. In contrast, Figure 3 (c) and (d) introduce increasing directional bias, particularly Figure 3 (d), where long-side openness (~24%) far exceeds that of the short side (~2.7%). Such asymmetry substantially lowers overall flow resistance but also promotes preferential flow pathways, increasing the likelihood of localized high-velocity regions and sheltered zones within the box.

Despite the well-established interactions between packaging geometry, airflow behaviour, and gas transport in other commodities, comparable investigations remain largely absent in the context of table grape packaging systems. Commercial table grape cartons display considerable variability in vent-hole configuration and distribution, as illustrated in Figure 3, yet the implications of these design differences for airflow penetration, cooling uniformity, and internal gas distribution have not been systematically evaluated. Consequently, current packaging practices rely largely on empirical design evolution rather than quantitative understanding of how carton geometry interacts with pallet airflow fields, internal packaging components, and fruit physiological responses. Addressing this knowledge gap is essential for interpreting how ventilation design influences not only cooling efficiency but also moisture loss, sulphur dioxide dispersion, and overall storage performance in commercial table grape cold chains.

## 2.5 Liners

Table grape liners constitute the principal internal resistance element within the carton–punnet–$SO_2$ pad assembly. While cartons govern macroscopic airflow and pallet-scale cooling heterogeneity[9, 42], liners regulate intra-carton convective exchange, diffusive gas transport, water vapour retention, and $SO_2$ dynamics. Their performance therefore emerges from coupled interactions among fruit transpiration, ventilation area, film permeability, airflow intensity, and $SO_2$ release kinetics. Based on functional design, liners can be categorized into non-perforated, macro-perforated, and micro-perforated systems.

View Article Online
DOI: 10.1039/D6FB00142D

### 2.5.1 Non-perforated liners

Early export systems frequently employed non-perforated low-density polyethylene (LDPE) liners to maximize relative humidity (RH) and reduce mass loss. Experimental multilayer-packaging studies demonstrated that severely restricted ventilation increases airflow resistance and slows moisture escape, thereby sustaining high in-package RH and reducing both berry mass loss and rachis dehydration.[33, 43] Non-perforated films were also shown to maintain elevated RH during forced-air cooling and early storage, resulting in lower physiological weight loss compared with perforated alternatives.[33]

Beyond humidity effects, restricted ventilation has direct implications for internal gas composition. Because gas transfer in sealed or low-vent liners is dominated by diffusion rather than convection, reduced permeability can alter the balance between fruit respiration and gas exchange. Packaging studies evaluating liners with different perforation areas demonstrate that reduced perforation fractions modify internal headspace gas concentrations, indicating that restricted gas exchange can lead to substantial atmosphere shifts inside the carton.[44] Recent packaging reviews similarly highlight that film permeability and vent configuration govern the movement of $O_2$, $CO_2$, and water vapor in table-grape packaging, and that low-vent systems can develop atmospheres that diverge from ambient conditions when respiration exceeds diffusive exchange.[14] Together, these findings indicate that sealed or minimally ventilated liners can accumulate $CO_2$, especially under conditions of low airflow and high metabolic activity.

Interactions between plastic liners and $SO_2$ pad systems further highlight the importance of gas exchange within packaged table grapes. Experimental studies have shown that the concentration and distribution of $SO_2$ within the package atmosphere depend strongly on the permeability and sealing characteristics of the liner, which regulate the rate of gas exchange between the package headspace and the surrounding environment.[39] When liners are poorly ventilated or tightly sealed, $SO_2$ released from the pad may accumulate within the enclosed atmosphere before diffusing out of the package, increasing the likelihood of localized overexposure.

While sustained low concentrations of $SO_2$ are necessary for effective decay suppression, excessive accumulation within the liner environment can increase the risk of berry bleaching and

View Article Online
DOI: 10.1039/D6FB00142D





rachis injury, particularly when free moisture is present on fruit surfaces. These interactions illustrate that liner design not only influences humidity retention and moisture loss but also governs the internal distribution and residence time of $SO_2$ within the package.

Taken together, the available studies indicate that liner ventilation area cannot be optimized based on a single performance criterion. Non-perforated systems maximize humidity retention and $SO_2$ residence time but impose significant resistance to airflow, limiting cooling efficiency and increasing the risk of $CO_2$ accumulation. Conversely, increasing perforation area enhances convective heat and mass transfer, improving cooling uniformity but reducing humidity control and $SO_2$ retention. The optimal ventilation configuration therefore represents a system-level compromise, dependent on fruit respiration kinetics, airflow conditions during precooling, and $SO_2$ release characteristics. Current commercial practices, which employ limited macro-perforation, implicitly reflect this trade-off; however, quantitative thresholds for optimal perforation area remain insufficiently defined and require integrated modelling approaches that couple gas exchange, airflow, and $SO_2$ dynamics.

### 2.5.2 Macro-perforated liners

Macro-perforated liners, typically incorporating 4–6 mm diameter holes with total ventilation areas between approximately 0.3% and 2.7% represent the current industry standard in many exporting regions.[44] The introduction of discrete perforations substantially reduces airflow resistance relative to sealed liners and improves cooling efficiency while maintaining high relative humidity.[9]

Lichter *et al.*[27] showed that controlled perforation enabled maintenance of high RH while preventing excessive $CO_2$ accumulation, resulting in improved rachis appearance. Fonseca *et al.*[45] demonstrated that steady-state $CO_2$ concentrations scaled with perforation area, indicating that mass transfer was dominated by hole geometry rather than intrinsic film permeability. Similarly, Ngcobo *et al.*[9] quantified airflow resistance through multi-scale table grape packaging and demonstrated that liner films contributed 40–83% of total pressure drop depending on perforation level, confirming that gas exchange under forced convection was governed primarily by total open area and hole diameter rather than fruit bulk characteristics. The trade-off between decay suppression and bleaching is well illustrated by[44]. Liners with low ventilation area (0.3%)

View Article Online
DOI: 10.1039/D6FB00142D

maintained higher $SO_2$ concentrations and reduced decay by 76.1% but induced 10.3% berry bleaching. Increasing ventilation area to 2.7% reduced bleaching to 0.5% but increased decay to 24.3%. These findings demonstrate that macro-perforated liner design constitutes a multi-objective optimization problem balancing $SO_2$ retention against gas exchange.

### 2.5.3 Micro-perforated liners

Micro-perforated liners employ smaller, more uniformly distributed perforations to achieve finer control of gas exchange. Compared to macro-perforated systems, they reduce airflow resistance while potentially allowing more stable atmospheric regulation. Amorim *et al.*[33] compared non-perforated, macro-perforated, and micro-perforated bags and reported that non-perforated liners minimized weight loss (4.84%) but required longer cooling times, whereas micro-perforated systems improved cooling and reduced berry abscission (0.43%) at intermediate pallet levels.[33] Ngcobo *et al.*[9] similarly observed reduced airflow impedance with perforated liners relative to sealed systems.[9] However, the impact of micro-perforation on rachis browning remains inconsistent across studies. Some trials indicate that reduced weight loss does not necessarily prevent rachis discoloration under extended storage, suggesting that rachis physiology responds to additional microclimatic variables beyond bulk humidity. Conversely, Raban *et al.*[46] reported reduced rachis browning in micro-perforated systems, highlighting the influence of cultivar, storage duration, and temperature stability.[46] Because micro-perforated systems are sensitive to temperature fluctuations and total ventilation area, their performance depends strongly on cold chain stability. Small changes in temperature can alter respiration-driven gas accumulation, potentially shifting equilibrium conditions.

### 2.5.4 Systematic MAP-guided liner design in table grapes

Despite extensive empirical evaluation of perforation area, airflow resistance, decay incidence, bleaching, and weight loss, liner selection in table grapes has rarely been derived from a predictive modified atmosphere packaging (MAP) framework grounded in respiration kinetics and mass-balance principles. Chen *et al.*[47] provided a clear example of such a framework in 'Kyoho' table grapes. Using measured $O_2$ consumption and $CO_2$ production rates, combined with film permeability data, they derived the required film thickness necessary to achieve a predefined

View Article Online
DOI: 10.1039/D6FB00142D



equilibrium atmosphere within safe physiological limits. Their approach was based on steady-state mass balance:

$$k_{O_2} A(O_{2,ext} - O_{2,in}) = R_{O_2}(T)\, m \quad (1)$$

$$k_{CO_2} A(CO_{2,in} - CO_{2,ext}) = R_{CO_2}(T)\, m \quad (2)$$

where $k_i$(m s$^{-1}$) represents the overall transfer coefficient (film + perforation + boundary layer), $A$ (m$^2$) represents effective exchange area, $m$ is fruit mass (kg), and $R_i(T)$ (mol kg$^{-1}$ s$^{-1}$) temperature-dependent respiration rates. For perforated liners, gas transfer through the polymer matrix and through perforations occurs in parallel, such that the overall transport capacity is the sum of film and perforation contributions (i.e., (kA)total = (kA)film + (kA)perf), while boundary layer resistances act in series with this combined pathway. The effective overall transfer coefficient $k_i$ is defined with respect to the total external area $A_{\text{total}}$:

$$k_i = \frac{(kA)_{\text{film}} + (kA)_{\text{perf}}}{A_{\text{total}}} \quad (3)$$

Expanding:

$$k_i = \frac{k_{\text{film}} A_{\text{film}} + k_{\text{perf}} A_{\text{holes}}}{A_{\text{total}}} \quad (4)$$

Here, $A_{\text{film}}$ and $A_{\text{holes}}$ represent the polymer-covered area and total perforation area, respectively, such that the overall transport capacity is given by the sum of pathway-specific conductance. The perforation contribution reflects combined diffusive and airflow-driven exchange through discrete openings and is therefore strongly influenced by perforation geometry and external airflow conditions.

Dividing the two mass balance relationships links internal $CO_2$ and $O_2$ via the respiratory quotient (RQ), demonstrating that equilibrium atmosphere is jointly determined by respiration kinetics and package transport properties. Importantly, Chen *et al.*[47] first defined a target $O_2$–$CO_2$ window to avoid anaerobic injury (<1–2% $O_2$) and excessive $CO_2$ damage (>10–15% $CO_2$, cultivar- and temperature-dependent), and only then derived packaging specifications from kinetics and permeability parameters. Experimental validation confirmed that model-derived film selection was more reliable than empirical trial-and-error approaches.

View Article Online
DOI: 10.1039/D6FB00142D

In contrast, most table grape liner studies vary perforation area (e.g., 0.3–2.7% ventilation area) and evaluate decay or bleaching outcomes post-storage, without first defining a cultivar-specific atmospheric target range or verifying whether the tested liner configuration satisfies respiration–diffusion balance constraints. Perforation number is therefore adjusted empirically rather than derived from mass-balance requirements.

From a mechanistic perspective, respiration in table grapes must be described within a coupled diffusion–reaction framework, in which internal gas transport and metabolic activity jointly determine headspace composition. At the fruit surface, gas exchange across the skin is governed by a first-order mass transfer boundary condition:

$$-D_{e,i}\frac{\partial C_i}{\partial n} = h_{i,\text{skin}}\left(C_i - C_{\text{ext},i}\right) \quad (5)$$

where $D_{e,i}$(m$^2$ s$^{-1}$) is the effective diffusivity within the tissue, $h_{i,\text{skin}}$ (m s$^{-1}$) is the skin mass transfer coefficient, $C_i$(mol m$^{-3}$) is the internal gas concentration, and $C_{\text{ext},i}$ (mol m$^{-3}$) is the corresponding headspace concentration. This boundary condition describes mass transfer across the fruit skin, linking internal diffusion within the tissue to gas exchange with the surrounding headspace. Within the fruit, respiratory gas exchange is governed by Michaelis–Menten-type kinetics distinguishing oxidative and fermentative pathways. The local oxygen consumption rate $R_{O_2}$and carbon dioxide production rate $R_{CO_2}$are expressed as:

$$R_{O_2} = -\frac{V_{m,O_2}\, C_{O_2}}{K_{m,O_2} + C_{O_2}} \quad (6)$$

$$R_{CO_2} = -r_{q,\text{ox}}\, R_{O_2} + \frac{V_{m,f,CO_2}}{1 + C_{O_2}/K_{m,f,O_2}} \quad (7)$$

where $V_{m,O_2}$and $V_{m,f,CO_2}$(mol m$^{-3}$ s$^{-1}$) are the maximum oxidative and fermentative respiration rates, respectively; $K_{m,O_2}$and $K_{m,f,O_2}$(mol m$^{-3}$) are the Michaelis–Menten constants describing oxygen affinity and fermentative inhibition; $C_{O_2}$(mol m$^{-3}$) is the local oxygen concentration; and $r_{q,\text{ox}}$ (–) is the respiratory quotient under fully aerobic conditions.[46] These expressions capture the transition from aerobic respiration to fermentative metabolism under low oxygen availability,

View Article Online
DOI: 10.1039/D6FB00142D



which is critical for defining safe atmospheric limits in table grape packaging. The temperature dependence of respiration is described using an Arrhenius relationship:

$$V_{m,i} = V_{m,i,\mathrm{ref}} \exp\left[\frac{E_{a,V_{m,i}}}{R}\left(\frac{1}{T_{\mathrm{ref}}} - \frac{1}{T}\right)\right] \quad (8)$$

where $V_{m,i,\mathrm{ref}}$ is the reference maximum rate at temperature $T_{\mathrm{ref}}$, $E_{a,V_{m,i}}$(J mol$^{-1}$) is the activation energy, $R$ is the universal gas constant, and $T$(K) is the absolute temperature. This formulation reflects the strong, non-linear sensitivity of respiration to temperature.

These kinetic expressions are coupled to gas transport within the fruit tissue through the diffusion–reaction equation:

$$\alpha_i \frac{\partial C_i}{\partial t} = \nabla \cdot \left(D_{e,i} \nabla C_i\right) + R_i \quad (9)$$

where $\alpha_i$represents the gas solubility capacity of the tissue and $R_i$ (mol m$^{-3}$ s$^{-1}$) is the reaction term defined by the respiration kinetics (Eqn. (6) and (7)). Together with the surface boundary condition, this formulation provides a physically consistent description of spatio-temporal gas dynamics in the fruit.

The conceptual structure of a predictive MAP-guided liner design strategy for table grapes is illustrated in Figure 4. The framework integrates (i) cultivar-specific respiration kinetics and safe atmospheric windows, (ii) steady-state mass-balance equations linking respiration to effective transfer coefficients, and (iii) liner design variables such as perforation geometry, film properties, and ventilation area. In this approach, liner specification is derived from predicted equilibrium gas composition rather than inferred from post-storage quality measurements. The figure also contrasts this mechanistic pathway with the commonly adopted empirical method, where perforation percentage is varied and evaluated retrospectively. Adoption of such a framework would reposition liner design as a constrained optimization problem embedded within the broader carton–pallet–cold chain system. Particularly under export conditions characterized by temperature variability and spatial airflow heterogeneity, a kinetics-based MAP design approach provides a rational basis

View Article Online
DOI: 10.1039/D6FB00142D

421 for selecting ventilation area and film properties that maintain internal atmospheres within
422 cultivar-specific safety limits.

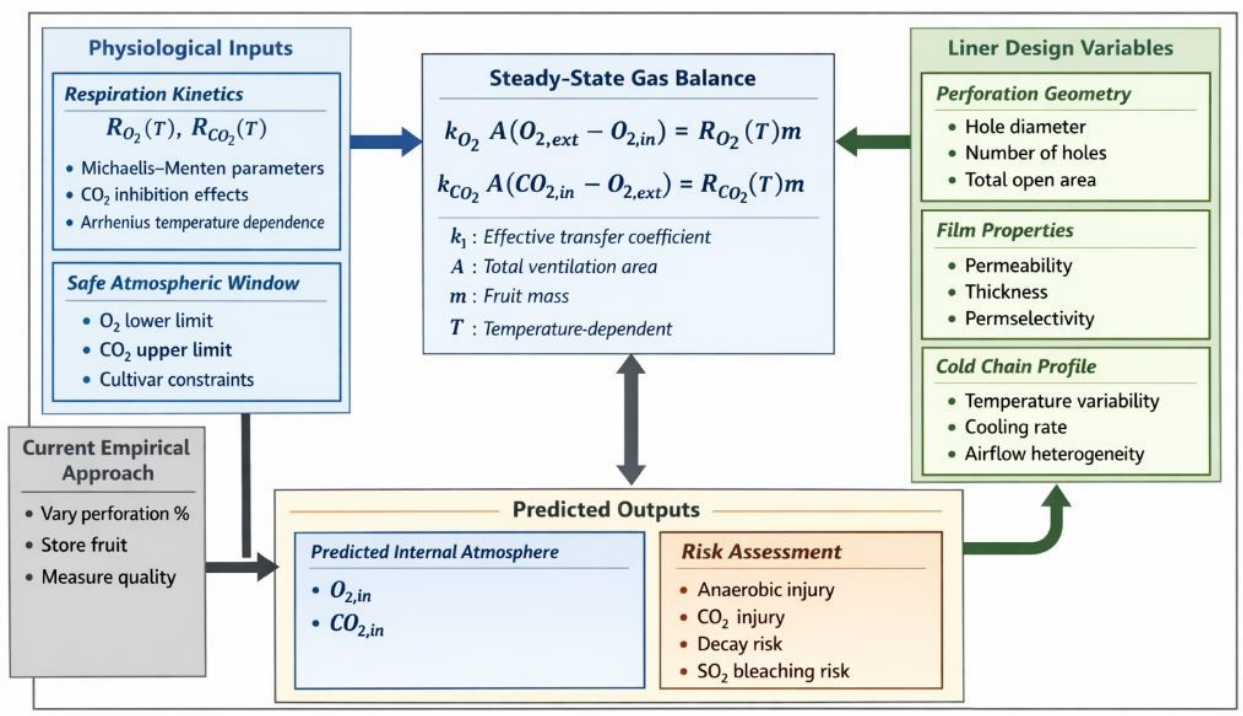

423

424 Figure 4: Conceptual framework for predictive MAP-guided liner design in table grapes.

425 **2.6 Sulphur dioxide ($SO_2$) technology in the table grape**

426 **2.6.1 Postharvest $SO_2$ application modes**

427 Sulphur dioxide ($SO_2$) has long been the primary technology used to control *Botrytis cinerea* in
428 commercial table grape cold chains, and it can be delivered through several postharvest application
429 modes. One approach is short-term fumigation, where grapes are exposed to relatively high
430 concentrations of gaseous $SO_2$ shortly after harvest to reduce microbial load and suppress surface
431 infections before packaging. Experimental studies have shown that carefully controlled fumigation
432 treatments can effectively reduce decay and pest incidence while maintaining acceptable fruit
433 quality when appropriate dose and exposure durations are applied.[13, 48, 49] However, because
434 fumigation provides only temporary protection, it is typically complemented by additional decay-
435 control strategies during long-distance storage and export.

View Article Online
DOI: 10.1039/D6FB00142D

In modern packaging systems, $SO_2$ is most commonly delivered through in-package $SO_2$-generating pads, which release the gas gradually within the package headspace during storage and transport. These pads are widely used because they provide sustained antifungal activity while maintaining the low-temperature and high-humidity conditions required to preserve fruit quality. Recent studies continue to confirm the effectiveness of pad-based $SO_2$ delivery in suppressing gray mold and maintaining commercial quality attributes in stored table grapes.[13] Variations in pad design, including slow-release and dual-release systems, are used to regulate the timing and intensity of $SO_2$ exposure during storage.

In addition to these two principal approaches, integrated strategies combining early postharvest $SO_2$ treatments with in-package delivery systems have also been explored to extend storage duration under commercial conditions.[48] Collectively, these approaches demonstrate that $SO_2$ application in table grape supply chains encompasses multiple delivery modes, each designed to balance effective decay control with the need to avoid excessive exposure that could lead to berry bleaching or quality deterioration. The mechanisms and performance of in-package $SO_2$ pad systems are discussed in greater detail in the following sections.

The comparative performance of these $SO_2$ delivery strategies across cultivars and storage conditions is summarized in Table 2. While the general efficacy of $SO_2$ is well established, the reported outcomes reveal substantial variability in response depending on cultivar sensitivity, storage duration, and delivery configuration, including the use of dual-release systems, modified atmospheres, and combined treatments. These studies collectively illustrate that optimization of $SO_2$ application is not solely a matter of dose, but of delivery dynamics and system context, which ultimately govern both decay control and quality preservation.

459 Table 2: Summary of reported effects of $SO_2$ delivery strategies on decay control and quality preservation in table grape cultivars

| Table grape cultivar | Treatment | Principal outcomes | References |
|---|---|---|---|
| 'Italia' | Field $SO_2$ application combined with dual-release $SO_2$ pads during cold storage (≈0–1 °C; up to 90 d) | Combined field and in-package $SO_2$ delivery reduced gray mold incidence and maintained cluster visual quality during long-term storage. | [50] |
| 'Italia' | Slow-release and dual-release $SO_2$ pads in clamshell packaging with micro-perforated liners (1 °C; 50 d + 7 d shelf life) | Dual-release pads provided superior gray mold control without significant changes in physicochemical quality; fast-reduced variants were effective for $SO_2$-sensitive cultivars. | 13 |
| 'BRS Nubia' | $SO_2$-generating pad during cold storage (2 °C, 30 days; ±*Botrytis cinerea* inoculation) | Gray mold incidence reduced by approximately 50% relative to untreated controls; quality attributes remained within acceptable limits. | 16 |
| 'Scarlotta Seedless' | $SO_2$-generating pads combined with ethanol treatment during extended cold storage (≈14 weeks) | Approximately 90% of clusters remained marketable after storage, with limited berry breakdown. | [51] |
| 'Red Globe' | Periodic $SO_2$ fumigation combined with modified atmosphere packaging (0–1 °C; up to 240 d) | Repeated low-dose fumigation effectively suppressed fungal development and preserved overall quality during very long storage. | [52] |
| 'Kyoho' | Constant $SO_2$ concentrations (≈28–57 mg $m^{-3}$) applied at different temperatures (0–25 °C) | Higher $SO_2$ concentrations were required to control decay at elevated temperatures, while lower concentrations were sufficient under cold storage. | [53] |
| 'BRS Vitoria' seedless | Slow-release, dual-release, and fast-reduced dual-release $SO_2$ pads during cold storage | Fast-reduced dual-release pads effectively controlled gray mold for up to 50 d, including in inoculated fruit | [54] |
| 'BRS Vitoria' | Dual-release $SO_2$ pads applied to *Botrytis cinerea*-inoculated grapes during cold storage | Gray mold was effectively suppressed without detrimental effects on berry quality | [55] |
| 'Kyoho' | Sustained-release $SO_2$ agents under simulated transport vibration (≈56 d storage) | $SO_2$ treatment reduced decay, berry abscission, and weight loss under both static and vibration conditions. | [49] |
| 'Sugrathirtyfive' seedless | Single-release vs. dual-release $SO_2$ pads under commercial cold storage (≈40 d) | No statistically significant differences in decay control or quality attributes between pad types under the tested conditions. | 26 |

View Article Online
DOI: 10.1039/D6FB00142D



### 2.6.2 $SO_2$-releasing pads system and the peak-dose problem

Emission studies indicate that $SO_2$-generating sheets typically exhibit dual-phase release behavior, consisting of an initial rapid release of $SO_2$ followed by a prolonged period of lower, sustained emission.[56] The early high-release phase contributes to rapid suppression of *Botrytis cinerea*; however, excessive transient $SO_2$ concentrations may cause localized injury such as berry bleaching and increased residue levels when exposure is not well controlled.[39] In conventional commercial configurations, $SO_2$ pads are positioned above the fruit beneath a plastic liner, which can create concentration gradients within the package. Under limited mixing conditions, the upper punnet or fruit layer may therefore experience the highest transient $SO_2$ dose.[14, 39] These interactions highlight the importance of packaging design and microclimate management in balancing effective decay suppression with the avoidance of $SO_2$ injury.

### 2.6.3 Intermediate barrier layer as a peak-exposure mitigation strategy in $SO_2$ pad systems

Figure 5 provides a modified configuration in which an intermediate porous barrier sheet is inserted between the $SO_2$-generating pad and the uppermost fruit layer. This additional step, illustrated in panel (c), represents a subtle but mechanistically important modification to the conventional packaging sequence described by de Aguiar *et al.*[14] In the conventional configuration, the $SO_2$-generating pad is placed directly above the packed fruit under a sealed liner. To this end, the shortest transport pathway from source to fruit coincides with the region of highest instantaneous concentration. In practice, fruit located closest to the $SO_2$ generator pad, typically the berries positioned at the top of the punnet, may experience the highest transient exposure during the early release phase.[39] Excessive $SO_2$ accumulation at these locations has been associated with berry surface bleaching and tissue injury, when exposure exceeds tissue tolerance.[48, 57] The insertion of an intermediate porous sheet, as shown in panel Figure 5 (c), modifies this source–fruit interface. Instead of direct pad-to-headspace transfer, the pathway becomes: "$SO_2$ pad → porous barrier → headspace → fruit surface". From a mass-transfer perspective, this introduces an additional diffusive resistance in series with the pad interface, thereby moderating the rate at which $SO_2$ enters the package headspace and reaches the fruit surface.

In addition to this transport effect, the porous barrier itself, typically a plant-based paper sheet, may interact with $SO_2$ through sorptive processes. Cellulose-based materials possess abundant

View Article Online
DOI: 10.1039/D6FB00142D



hydroxyl functional groups and porous microstructures that enable adsorption of various gases and pollutants.[58, 59] Consequently, the barrier may function not only as a diffusion resistance but also as a partial sink that attenuates transient concentration peaks above the fruit layer. Similar coupled processes of convection, diffusion, and adsorption have been reported for other postharvest gases, including 1-methylcyclopropene (1-MCP), where interactions with materials and biological tissues influence gas distribution within storage environments.[18] However, the extent to which plant-based barrier sheets absorb or buffer $SO_2$ within table grape packages remains largely unquantified, and the overall mass balance of $SO_2$ among the gas phase, fruit tissues, and packaging materials has received limited attention in the literature.

The barrier effect cannot be evaluated in isolation. Liner perforation density and carton vent alignment govern convective exchange and $SO_2$ retention.[14] Higher air velocities during forced-air precooling may reduce stratification but also increase convective $SO_2$ loss; conversely, unperforated liners may improve retention but elevate condensation risks. Accordingly, barrier insertion is best viewed as a controllable "dose-shaping" element within the broader pad–liner–vent system.

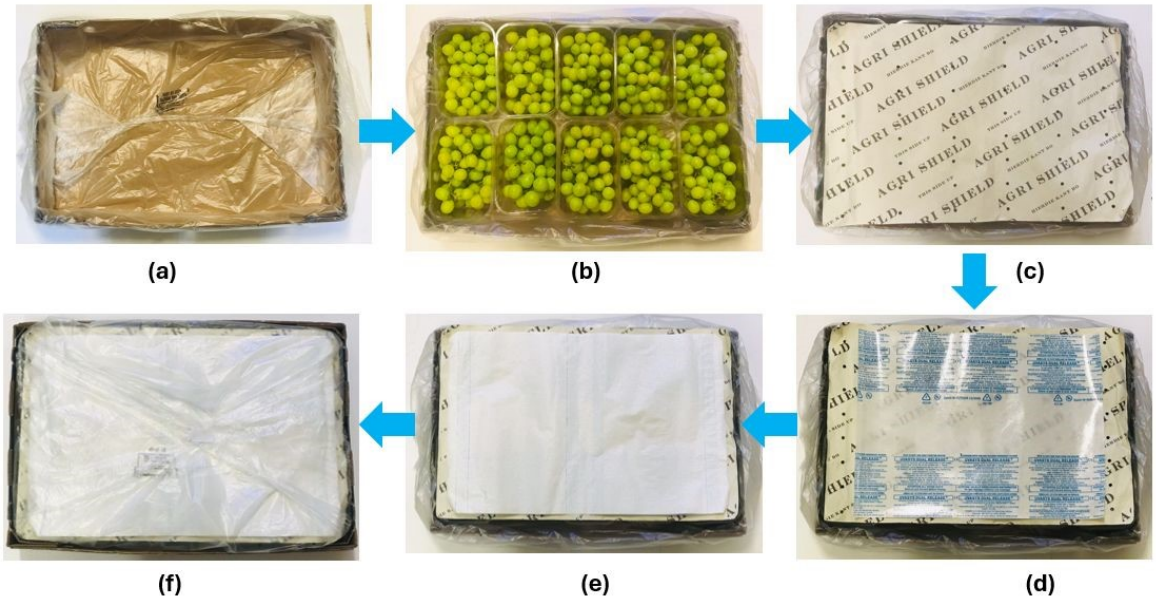


Figure 5 Packaging sequence illustrating incorporation of an intermediate barrier sheet between the fruit and an $SO_2$-generating pad in a table grape export carton. (a) Perforated plastic liner inserted into the carton. (b) Punnets loaded with grapes. (c) Intermediate barrier sheet placed directly on top of the punnets (barrier insertion step). (d) $SO_2$-generating pad positioned on top of the barrier sheet. (e) Moisture-absorbing sheet placed above the pad assembly. (f) Liner sealed to complete the package microenvironment. Arrows

View Article Online
DOI: 10.1039/D6FB00142D

indicate the operational sequence; panel (c) highlights the barrier step that distinguishes this configuration from the conventional pad-on-top system commonly used in commercial practice and described by de Aguiar et al. (2023).

## 2.7 Punnet and clamshells in table grapes packaging

Retail-ready punnets and clamshells are the dominant internal packaging format in export-oriented table grape supply chains, replacing bulk loose-pack systems in many markets because of improved unit protection, traceability, and consumer handling convenience.[31, 43] However, beyond these commercial drivers, punnet and clamshell geometry plays an active role in governing heat transfer, moisture dynamics, and $SO_2$ redistribution within export cartons.

Figure 6 illustrates a representative clamshell design (≈160 mm × 90 mm footprint) (Figure 6 (a)), showing discrete circular and slot vents in the lid (e.g., Ø10 mm and 5 mm perforations), Figure 6 (b) shows a punnet with sidewall circular Ø8 mm vent openings (~21 mm spacing). Both clamshells and punnets usually have reinforced ribbed sidewalls. These geometric features define the effective open area ratio, internal headspace volume, and airflow resistance of the retail unit. Because punnets are arranged in arrays within vented cartons, their orientation and vent alignment relative to carton vents influence convective heat removal and gas exchange during both precooling and storage.[20, 43]

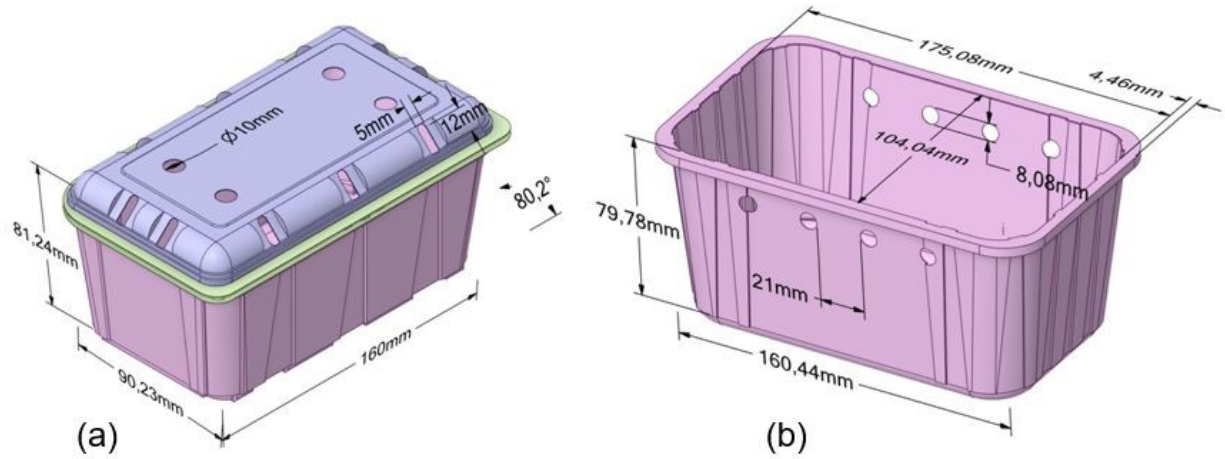


Figure 6: Representative geometry of a vented table-grape clamshell (a) and punnet (b) unit. Dimensions show a typical retail scale (160 mm × 90 mm footprint).

View Article Online
DOI: 10.1039/D6FB00142D



A characteristic feature visible in the Figure 6 is the presence of vertical grooves or ribs along the sidewalls of the punnet. These grooves increase the external surface area relative to a smooth-walled container. From a heat transfer perspective, increasing external surface area enhances the available area for convective heat exchange. Although few table grape studies isolate the effect of punnet rib geometry specifically, packaging-level cooling investigations consistently show that airflow distribution and exposed surface area influence temperature uniformity and cooling time within cartons.[20, 43] Therefore, ribbed punnet surfaces should not be considered purely structural reinforcements; they may contribute to enhanced local convective exchange and turbulence generation at the micro-scale.

### 2.7.1 Vent architecture: circular side holes and lid perforations

Figure 6 highlights the circular side-wall vents common in commercial punnets, typically four openings along each long side. Along with lid perforations, these vents determine the resistance between the carton headspace and the punnet interior. Vent diameter, spacing, and total open area define airflow pathways and strongly influence heat- and mass-transfer behaviour. Experimental and computational studies show that vent-hole ratio and vent alignment modify airflow resistance and cooling efficiency in punnet and clamshell systems. Larger or more numerous openings reduce pressure drop and improve cooling rate during forced-air precooling.[43] Vent geometry also influences internal humidity and gas exchange during storage, with permeability and vent area affecting how rapidly vapour conditions equilibrate between carton and punnet.[43]

Ventless punnets are used in some supply chains to promote humidity retention and reduce rachis dehydration. Because rachis tissue exhibits higher transpiration and contributes disproportionately to visible quality loss, reduced airflow can reduce local vapour-pressure deficit and slow browning.[2, 31] However, smaller vent area increases airflow resistance and may slow cooling, modify $SO_2$ penetration kinetics, and increase condensation sensitivity during temperature fluctuations.[14, 44]

In contrast, fully vented punnets facilitate rapid heat removal and more uniform gas equilibration but may increase moisture loss when carton-level RH is not adequately controlled. Although several studies quantify vent-related differences in airflow resistance and cooling, direct

View Article Online
DOI: 10.1039/D6FB00142D



559 comparisons of vented versus ventless punnets under extended export simulation remain limited.
560 Consequently, commercial practice often reflects empirical preference rather than mechanistically
561 optimised design criteria.[43]

562 ### 2.7.2 Interaction with $SO_2$ peak-dose dynamics

563 Punnet vent architecture directly influences the propagation of early $SO_2$ peaks from the pad into
564 individual retail units. In the conventional pad-on-top system[14], early biphasic release may create
565 transient high concentrations near the top carton layer[56]. If punnet lid vents are large and directly
566 aligned with the source, equilibration may be rapid, increasing top-layer exposure. If vent area is
567 limited, internal diffusion may delay equilibration but potentially increase heterogeneity within
568 the punnet. When an intermediate porous barrier is inserted between pad and fruit (as discussed in
569 the preceding subsection), the resistance network expands: (Pad→Barrier→Carton headspace→
570 Punnet vents→Berry surface). In this system, punnet vent geometry determines how effectively
571 attenuated $SO_2$ flux redistributes within each retail unit.[41] Thus, punnet design cannot be decoupled
572 from pad placement strategy in evaluating peak-dose risk and exposure uniformity.

573 Punnet and clamshell packaging should be regarded as multi-functional microenvironment
574 regulators. Their ribbed surfaces influence convective heat transfer area; their vent architecture
575 governs airflow resistance, cooling rate, humidity retention, and $SO_2$ penetration; and their
576 structural rigidity maintains geometric stability under pallet loads. Despite their central role in
577 determining cooling performance, water loss dynamics, and $SO_2$ exposure patterns, systematic
578 comparative data on vented versus ventless designs under realistic export conditions remain
579 limited. Given the demonstrated sensitivity of rachis tissues to VPD and of fruit surfaces to
580 transient $SO_2$ peaks[27], further mechanistic evaluations of punnet geometry represent an important
581 opportunity for optimizing postharvest performance in export-oriented table grape supply chains.

582 # 3 Innovative packaging technologies for table grapes

583 ## 3.1 The central role of $SO_2$ in table grape storage

584 Packaging innovation in table grape systems is strongly shaped by the need to control postharvest
585 decay and maintain rachis quality during extended cold storage and long-distance export. Among

View Article Online
DOI: 10.1039/D6FB00142D



postharvest challenges, decay caused primarily by *Botrytis cinerea* remains the dominant storage problem, while rachis browning is widely recognized as the second most important quality limitation affecting marketability.[31] Because of these dual constraints, $SO_2$-based technologies have become indispensable in commercial table grape storage systems, as they effectively suppress fungal decay while also contributing to the mitigation of rachis browning and the preservation of bunch appearance during storage and transport.[14, 31, 39]

In commercial export systems, $SO_2$ delivery is typically integrated with packaging configurations that include liner bags, carton ventilation features, and palletized airflow pathways. These components collectively regulate humidity retention, gas diffusion, and fumigation effectiveness within packed fruit environments.[9, 43, 44] Consequently, packaging functions not only as a structural containment system but also as a microenvironmental regulator that governs mass transfer, gas distribution, and microbial suppression during storage and transport.

Despite the effectiveness of $SO_2$-based preservation, increasing attention has been directed toward packaging innovations that may complement or partially replace conventional approaches. These developments aim to enhance microbial suppression, regulate physiological responses, reduce moisture loss, and improve compatibility with evolving sustainability requirements and export logistics. Emerging strategies therefore focus on active packaging technologies, diffusion-modifying edible coatings, atmospheric manipulation, and biodegradable packaging materials, each seeking to improve the interaction between packaging systems and fruit physiology.

### 3.2 Active packaging systems: antimicrobial and ethylene-modulating approaches

Active packaging technologies introduce functional compounds into films, coatings, or sachets to suppress fungal growth or modulate physiological responses. Essential oil–based systems have

View Article Online
DOI: 10.1039/D6FB00142D



been widely investigated for antifungal efficacy against *Botrytis cinerea*. Oils such as oregano, cinnamon, thyme, clove, and neem exhibit inhibitory effects and have been incorporated into polymer matrices or vapor-phase systems.[60-62] Yun *et al.*[63] used composite essential oil microcapsules (CEOM) incorporated into biodegradable PCL/PLLA films combined with passive modified atmosphere packaging (PMAP). It extended the shelf life of table grapes from 12 days (control) to 28 days at 12°C storage, more than doubling the duration (~133% extension), while maintaining optimal gas levels (e.g., ~6.4% $O_2$ and 14% $CO_2$), significantly reducing spoilage microbes (e.g., fungal counts halved, major pathogens like Penicillium and Rhizobium suppressed), and preserving overall quality.

Despite promising antifungal performance, several limitations constrain commercial adoption. Essential oil volatility and release kinetics are highly temperature-dependent, potentially leading to rapid depletion or uneven distribution within cartons. Compatibility with $SO_2$ pads remains uncertain, as synergistic or antagonistic effects between antifungal vapors and sulphur dioxide have not been systematically quantified. Moreover, sensory thresholds and potential flavor tainting remain critical concerns for export markets.

Ethylene-modulating technologies represent another active packaging strategy. Although table grapes are considered non-climacteric, rachis senescence is influenced by ethylene sensitivity. Soldateli *et al.*[64] demonstrated that 1-MCP treatment significantly improved rachis visual quality, even when berry appearance remained largely unaffected.[64] These findings suggest that targeted ethylene inhibition may complement traditional $SO_2$-based decay control, particularly in long-distance supply chains where rachis browning determines market acceptance. However, integration with modified atmospheres and fumigation regimes requires further mechanistic evaluation.

Overall, active packaging strategies demonstrate potential but remain insufficiently integrated with mass-transfer modelling and pallet-scale airflow dynamics.

### 3.3 Edible coatings and surface modulation technologies

Edible coatings have been investigated as diffusion-modifying barriers that reduce transpiration, delay senescence, and enhance antimicrobial resistance. Chitosan-based coatings, alone or

View Article Online
DOI: 10.1039/D6FB00142D

combined with polysaccharides, have shown improvements in firmness retention and decay suppression. Eshghi *et al.*[65] reported that chitosan–gum ghatti coatings improved postharvest quality attributes, while Melo *et al.*[66] demonstrated chitosan nanoparticles (eco-friendly/edible) delaying ripening, reducing weight loss/soluble solids increase (linked to softening), minimizing decay/microbial growth, and preserving overall quality (including reduced browning/softening indicators) in table grapes during cold storage.

Mechanistically, edible coatings alter surface resistance to water vapor and gas diffusion, thereby modifying internal $O_2$ and $CO_2$ gradients. However, few studies quantify effective diffusivity changes or integrate coating permeability into respiration–diffusion models. Without such quantification, predicting internal atmospheric shifts under variable temperature regimes remains challenging. Additionally, coating uniformity on complex grape clusters introduces variability that is seldom addressed in experimental design.

### 3.4 Modified atmosphere and high-$CO_2$ interventions

Modified atmosphere packaging (MAP) and controlled atmosphere (CA) systems regulate $O_2$ and $CO_2$ concentrations to slow respiration and suppress microbial growth. Conventional MAP approaches increase $CO_2$ and reduce $O_2$ through passive equilibration, while CA storage actively controls atmospheric composition.[67] Beyond traditional respiration suppression, short-term high-$CO_2$ treatments have been shown to induce physiological tolerance. Rosales *et al.*[37] demonstrated that exposure to 20 kPa $CO_2$ for three days significantly reduced rachis browning, relative water content decrease during 33 days of storage at 0 °C. These treatments appear to enhance membrane stability and stress tolerance rather than merely suppress respiration.

However, the practical implementation of cyclic $CO_2$ treatments introduces operational complexity. Additional chamber requirements, timing control, and workflow adjustments may limit scalability in high-throughput export operations. Compared to passive $SO_2$ sheet application, controlled $CO_2$ cycling demands infrastructure and precision that may not be feasible in all supply chains.

Similarly, Cefola and Pace[68] demonstrated that high-$CO_2$ MAP (10% $CO_2$ with 20% $O_2$) effectively preserved organic ‘Italia’ grapes without sulphur dioxide during short-term storage.

View Article Online
DOI: 10.1039/D6FB00142D

While promising for niche organic markets, the stability of such atmospheres under fluctuating export temperatures remains uncertain.

These findings suggest that atmospheric interventions can substitute or complement $SO_2$ under controlled conditions, but their robustness under real export variability requires further modelling and validation.

### 3.5 Biodegradable materials

Indumathi *et al.*[69] explored biodegradable packaging by testing bio-based polysaccharide films, finding them effective in preserving table grape quality. These biodegradable materials align with growing sustainability demands, offering viable alternatives to conventional plastics. However, the balance between ecological benefits, cost-effectiveness, and compatibility with current $SO_2$ fumigation protocols remains a research gap.

Amorim *et al.*[33] emphasized the critical role of packaging liners in managing moisture and cooling dynamics for table grapes. Their study found that while unperforated liners maintained the highest relative humidity (RH), they also resulted in the longest cooling times. Furthermore, the level of palletization was shown to influence both temperature and RH. However, the long-term implications of liner selection and its interaction with variable environmental conditions remain underexplored, representing a key opportunity for future optimization.

Active packaging systems, particularly those incorporating ethylene absorbers or reducers, show significant promise for extending grape shelf-life. This potential was demonstrated by Soldateli *et al.*[64] who found that while 1-MCP (a common ethylene inhibitor) had a minimal effect on berry appearance, it significantly improved the visual quality of the rachis during storage. Such technologies are especially valuable for long-distance supply chains where maintaining quality is critical. However, further research is essential to fully understand their interactions with grape physiology and to integrate them effectively with established preservation methods like $SO_2$ generator pads.

View Article Online
DOI: 10.1039/D6FB00142D

Innovative packaging design is pivotal for optimizing airflow, improving cooling rates, and reducing postharvest spoilage. South African table grapes, destined for distant export markets, could benefit significantly from these enhancements.

# 4 Mathematical modelling and simulation in cold chain optimization

Mathematical modelling and simulation have increasingly been used as analytical tools to investigate transport processes within fresh produce cold chains. These approaches extend beyond descriptive quality assessments and enable mechanistic analysis of airflow distribution, heat transfer, gas diffusion, moisture loss, and fungicide dynamics within carton–pallet–container systems. However, modelling efforts in table grapes remain fragmented, typically focusing on isolated components rather than integrated packaging–physiology systems. The dominant modelling domains in table grape cold chain research include: (i) packaging box design, (ii) plastic liner behaviour, (iii) $SO_2$ pad release and distribution, and (iv) airflow and cooling rate uniformity.

## 4.1 Packaging box design and structural performance

Carton design influences airflow pathways, cooling efficiency, and mechanical stability within palletized produce systems. Computational fluid dynamics (CFD) studies by Ambaw *et al.*[6] and Ngcobo *et al.*[9, 43] demonstrated that vent hole size, position, and alignment can significantly affect airflow distribution within pallets. Poor vent alignment reduces convective heat removal and may contribute to cooling heterogeneity and localized condensation risks. Complementing these airflow investigations, A study that applied finite element analysis (FEA) to evaluate stress distribution in ventilated corrugated packaging, identified structural weaknesses that may lead to mechanical damage during handling and transport.[70] Such modelling approaches provide valuable insight into packaging durability and mechanical integrity.

View Article Online
DOI: 10.1039/D6FB00142D





However, the relative importance of carton ventilation design in table grape systems differs from that observed in other fruit industries such as pome fruit or citrus. In commercial table grape packaging, the presence of plastic liner bags, $SO_2$ generator pads, and internal packing configurations substantially alters airflow resistance and gas diffusion pathways within cartons. These components often act as dominant regulators of the package microenvironment, partially masking the influence of carton vent geometry on cooling behaviour and internal airflow patterns. Consequently, airflow and heat transfer dynamics in table grape systems are governed not only by carton design but also by the combined resistance imposed by liners and internal packaging elements.

Furthermore, most packaging box modelling studies evaluate airflow behaviour or mechanical resistance independently, without explicitly linking design modifications to downstream physiological outcomes such as decay kinetics, rachis browning, or $SO_2$ injury. This separation limits the predictive capacity of modelling frameworks for quality preservation. Future modelling efforts therefore require integrated carton–liner–fruit system analysis, where structural performance, airflow pathways, and physiological responses are considered simultaneously to better represent the complexities of commercial table grape cold chains.

### 4.2 Plastic liner modelling and gas–moisture transfer

Plastic liners introduce an additional resistance layer that alters convective airflow and diffusive gas exchange. Delele *et al.*[20] conducted 3D CFD simulations incorporating liner configurations and demonstrated that non-perforated liners prolonged cooling times and increased condensation risk.[20] Perforated liners improved airflow and reduced moisture accumulation under high-humidity conditions.

View Article Online
DOI: 10.1039/D6FB00142D





However, most liner modelling efforts focus primarily on airflow impedance and cooling time. Few studies integrate liner mass transfer behaviour with respiration-driven gas accumulation using steady-state or transient diffusion–reaction frameworks. As discussed in Section 2.5.4, systematic MAP-liner design remains largely absent in modelling studies, despite the feasibility demonstrated in kinetics-based packaging design literature.

Furthermore, liner modelling is often performed under steady temperature assumptions, while export cold chains experience dynamic thermal profiles that alter both respiration and effective mass transfer coefficients.

### 4.3 $SO_2$ pad release modelling and distribution dynamics

$SO_2$ generator pads are critical for decay control, yet their interaction with packaging geometry and airflow has been under-modelled relative to their commercial importance. Experimental studies show that ventilation resistance strongly affects $SO_2$ concentration distribution and bleaching risk.[39, 44] However, quantitative modelling of $SO_2$ release kinetics coupled with airflow and absorption remains limited. Few modelling efforts incorporate pad release rate kinetics, $SO_2$ diffusion within liner-constrained systems, spatial heterogeneity across pallet positions and $SO_2$ sorption by fruit and packaging materials. Without coupling $SO_2$ transport to airflow and liner mass transfer, predictive control of fungistatic concentration versus bleaching thresholds remains incomplete.

#### 4.3.1 Mechanistic basis for modelling $SO_2$ release and distribution

To moderate localized effects without compromising decay control, some packers introduce a porous intermediate barrier (Figure 5, (c)) between the $SO_2$ pad and the punnets. Although specific material properties of barrier sheets are not yet documented in the peer-reviewed literature, its functional role can be understood as an added diffusive resistance that reshapes peak exposure. In

View Article Online
DOI: 10.1039/D6FB00142D

a carton system without a barrier, the transient molar flux from pad to headspace can be approximated as:

$$J_0(t) = k_0 A\left(C_{pad}(t) - C_{hs}(t)\right) \quad (10)$$

where $J_0(t)$ is the molar flux (mol s $^{-1}$), $k_0$ is an effective mass transfer coefficient (m s $^{-1}$), $A$ is transfer area (m $^2$), $C_{pad}(t)$ is near-pad $SO_2$ concentration (mol m$^{-3}$), and $C_{hs}(t)$is headspace concentration (mol m$^{-3}$). This formulation represents a lumped, one-dimensional approximation in which transport across the pad–headspace interface is assumed to be diffusion-dominated. Convective effects associated with airflow within the carton (e.g., during forced-air cooling or storage ventilation) are not explicitly resolved but are incorporated implicitly within the effective coefficient $k_0$. As such, this expression captures first-order release dynamics rather than spatially resolved transport.

With the introduction of an intermediate porous layer, the flux can be expressed in resistance form:

$$J(t) = \frac{A\left(C_{pad}(t) - C_{hs}(t)\right)}{R_{pad} + R_{shield}} \quad (11)$$

$$R_{pad} = \frac{1}{k_0} \quad (12)$$

$$R_{shield} = \frac{L}{D_{e,shield}} \quad (13)$$

where $J(t)$ is the molar flux (mol s$^{-1}$), $R_{pad}$ and $R_{shield}$ are mass transfer resistances (s m$^{-1}$), $L$ is the barrier thickness (m), and $D_{e,shield}$ is the effective diffusivity of the barrier material (m$^2$·s$^{-1}$). The barrier thus introduces an additional resistance in series with the pad–headspace transfer pathway, reducing the net flux, particularly during the early high-release phase. The headspace concentration $C_{hs}(t)$ is treated as a spatially averaged, time-dependent variable (mol m$^{-3}$), governed by a transient mass balance that accounts for pad release, exchange with the external environment (ventilation losses, mol s$^{-1}$), and interactions with the fruit (absorption and chemical reactions, mol·s$^{-1}$). In this sense, the present formulation provides a reduced-order representation of $SO_2$ dynamics, while more detailed airflow and spatial distribution effects can be addressed through a detailed and airflow and mass transfer coupled CFD-based analyses. Overall, the introduction of a porous barrier reduces peak local concentrations near the top layer

View Article Online
DOI: 10.1039/D6FB00142D

(mitigating bleaching risk) while maintaining a more sustained $SO_2$ availability for decay suppression, consistent with observations reported by Lichter *et al*. [37]

### 4.3.2 Efficient representation of intermediate barrier sheets

For carton- and pallet-scale simulations, explicitly resolving a thin, porous sheet may be impractical. A pragmatic alternative is a flux modulation formulation:

$$J(t) = J_{pad}(t) \cdot f_{shield}(t) \quad (14)$$

where $J_{pad}(t)$is the measured pad emission pattern (Kaplunov *et al*.[56]) and $f_{shield}(t) \in (0,1]$captures attenuation. For early-time diffusion attenuation:

$$f_{shield}(t) = \exp\left(-\frac{L}{D_{e,shield}t^{1/2}}\right) \quad (15)$$

This representation can be coupled with CFD or finite-volume transport models to predict spatio-temporal $SO_2$ gradients and evaluate how barrier insertion alters peak exposure zones without requiring micro-scale meshing.

## 4.4 Airflow distribution, cooling rate, and thermal uniformity

Airflow and cooling rate modelling represent the most developed modelling domain in table grapes. CFD simulations consistently show significant heterogeneity within pallets and containers.[6, 43] Sidewall venting, vent alignment, and pallet arrangement strongly influence cooling time and temperature gradients. Fedeli *et al.*[5] used sensor-derived container data to identify systematic hotspot formation in export shipments from South Africa.[5] Hotspots were more frequent in upper container regions and near container doors, highlighting the impact of airflow distribution and operational practices. Such findings validate modelling predictions of spatial non-uniformity.

Thermal property modelling also supports cooling system design. Akhijahani and Khodaei[71] quantified temperature-dependent specific heat and thermal conductivity of 'Rasa' grapes, enabling improved parameterization of heat transfer models. Nevertheless, most airflow studies

View Article Online
DOI: 10.1039/D6FB00142D

focus on cooling time reduction rather than explicitly linking temperature gradients to physiological disorder risk or gas accumulation dynamics. The coupling between thermal heterogeneity and respiration-driven atmosphere shifts remains underexplored.

### 4.5 Toward integrated digital twin approaches

Modelling efforts in fresh produce cold chains have traditionally evolved along disciplinary lines, with structural mechanics, airflow simulation, gas diffusion, and quality kinetics often treated as independent analytical problems. This compartmentalization is not unique to table grapes; rather, it reflects the broader historical development of packaging and cold chain modelling, where thermal analysis, mass transfer, and mechanical performance were addressed separately according to available tools and expertise. However, the need for integration is arguably more critical in table grape systems than in many other commodities. The coexistence of multilayer packaging (carton–punnet–liner), deliberate atmospheric modification, and active $SO_2$ release creates tightly coupled thermal and mass transfer processes that cannot be adequately understood in isolation.

Structural finite element analyses have improved tray and carton durability, yet vent geometry influences not only mechanical integrity but also airflow pathways and convective heat transfer. Similarly, computational fluid dynamics (CFD) studies have successfully characterized pallet-scale airflow heterogeneity and cooling performance, but they rarely incorporate respiration-driven gas accumulation or humidity dynamics within liner-constrained environments. Liner investigations frequently focus on airflow impedance or perforation percentage without embedding these parameters within respiration–diffusion balance frameworks that predict internal $O_2$ and $CO_2$ levels. Modelling of $SO_2$ distribution, although experimentally recognized as sensitive

View Article Online
DOI: 10.1039/D6FB00142D

to ventilation resistance and temperature, is seldom coupled to spatial airflow fields or dynamic gas exchange through perforated liners.

Table 3: Current modelling focus in table grape cold chains and key missing couplings

| Modelling domain | Typical research focus | Common tools | Key outputs | Missing couplings / limitations | Representative sources |
|---|---|---|---|---|---|
| Airflow & Cooling | Vent design, pallet airflow, cooling time | CFD | Temperature maps, cooling rate | Rarely linked to respiration-driven gas shifts or $SO_2$ distribution | 9, 20, 43 |
| Packaging Structure | Mechanical stress, tray durability | FEA | Stress/strain fields | Vent geometry not jointly optimized with airflow & gas exchange | 41, 6 |
| Plastic Liners | Perforation %, airflow impedance | CFD, empirical testing | Cooling time, weight loss | Limited use of respiration–diffusion mass balance; MAP windows not systematically applied | 12, 11, 9, 20, 43 |
| $SO_2$ Pads | Decay suppression, bleaching risk | Experimental, limited diffusion modelling | $SO_2$ concentration | Rarely coupled with airflow field or liner-derived transfer coefficients | 27, 17, 21 |
| Thermal Properties | Specific heat, conductivity | Regression models | Parameter estimation | Not integrated into full airflow–respiration models | 18, 19, 8 |
| Sensor Systems | Temperature, $O_2$/$CO_2$/$SO_2$ tracking | IoT systems | Real-time monitoring | Often diagnostic only; limited predictive feedback integration | 5, 76,72, 23 |

In table grape systems, these interactions are particularly consequential. Airflow determines the temperature field, which in turn modulates respiration kinetics and thus internal gas composition. Liner ventilation area governs both $CO_2$ accumulation and $SO_2$ retention, linking decay suppression to bleaching risk. Temperature heterogeneity across pallet positions further amplifies these couplings, as respiration increases non-linearly with temperature while effective mass transfer coefficients may also shift. The presence of $SO_2$ pads adds an additional reactive species whose concentration depends simultaneously on airflow intensity, liner resistance, absorption by fruit tissue, and storage temperature. The result is a multiphysics system in which thermal, diffusive, and biochemical processes interact across spatial scales.

View Article Online
DOI: 10.1039/D6FB00142D





An integrated digital twin framework would explicitly connect temperature-dependent respiration kinetics, convective airflow distribution, diffusive mass transfer through liners, $SO_2$ release and absorption dynamics, and pallet-scale thermal variability within a unified predictive environment. Such a model would simulate spatial distributions of $O_2$, $CO_2$, relative humidity, $SO_2$ concentration, and temperature across cartons and pallet positions under realistic export conditions. By assimilating real-time sensor data, the digital twin could continuously update boundary conditions and identify deviations from safe atmospheric or thermal windows before physiological disorders manifest.

For table grapes, where quality preservation depends on a narrow balance between decay control and injury avoidance, integration is not merely an academic refinement but a practical necessity. The combination of multilayer packaging, active fumigation, and extended maritime transport amplifies the consequences of small modelling omissions. Moving from compartmentalized simulations toward system-level digital twins would therefore shift cold chain management from retrospective quality assessment to predictive design and proactive risk mitigation, supporting more robust export performance under variable commercial conditions.

The compartmentalized nature of current modelling efforts is summarized in Table 3, which highlights that airflow, structural integrity, liner mass transfer, and $SO_2$ release are typically investigated in isolation. Critical couplings-such as the interaction between airflow-induced temperature gradients and respiration-driven gas accumulation, or between liner ventilation resistance and $SO_2$ distribution kinetics, remain weakly integrated

The multiphysics interactions described above are synthesized conceptually in Figure 7, which positions fruit physiology at the core of the modelling framework and illustrates how airflow,

View Article Online
DOI: 10.1039/D6FB00142D

carton geometry, liner mass transfer, and $SO_2$ release dynamics are thermally and diffusively coupled. The figure emphasizes that airflow-induced temperature gradients modify respiration kinetics, liner geometry governs internal gas accumulation, and $SO_2$ distribution depends simultaneously on ventilation resistance and temperature. The outer digital twin layer represents the integration of sensor-derived data streams with mechanistic models, enabling dynamic updating of internal atmosphere and quality risk predictions. Together, the framework underscores the necessity of system-level integration for table grape cold chains, where multilayer packaging and active $SO_2$ application amplify cross-domain interactions.

View Article Online
DOI: 10.1039/D6FB00142D



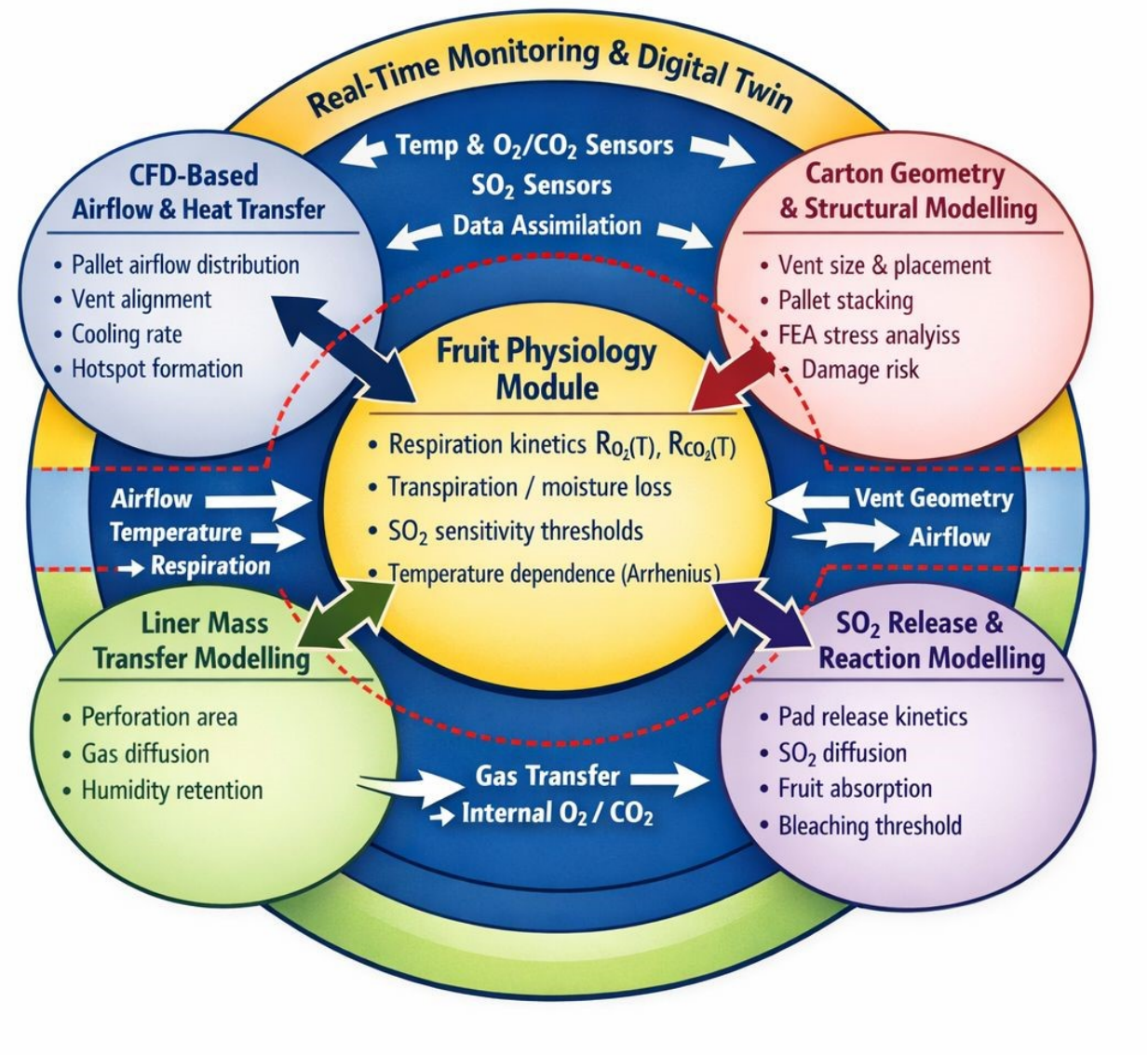


867

868 Figure 7: Schematic of an integrated multi-physics modelling framework for $SO_2$-based fungicide
869 management in table grape cold chains, comprising coupled sub-models for fruit physiology, CFD-based
870 airflow and heat transfer, liner mass transfer, $SO_2$ release and reaction kinetics, and carton geometry,
871 embedded within a real-time monitoring and digital twin architecture.

872 **4.6 Real-time monitoring and model validation**

873 The increasing deployment of sensor technologies in table grape supply chains has significantly
874 enhanced the capacity to monitor and document environmental conditions during storage and
875 transport. Temperature, relative humidity, and gas composition ($O_2$, $CO_2$, $SO_2$) are now routinely
876 measured in real time, enabling improved traceability, regulatory compliance, and postharvest

View Article Online
DOI: 10.1039/D6FB00142D

decision-making. However, beyond compliance and diagnostics, sensor integration provides a critical opportunity to validate and refine mechanistic cold-chain models under commercial conditions.

Poeta *et al.*[23] demonstrated the application of advanced nanosensor technology in controlled atmosphere (CA) storage of 'Italia' table grapes. Their study compared optimal CA conditions (3% $O_2$ / 10% $CO_2$) with high-$CO_2$ stress (3% $O_2$ / 30% $CO_2$) and ambient air storage, using an S3+ electronic nose equipped with $SnO_2$-based metal oxide semiconductor (MOS) sensors doped with Pd/Au. Real-time volatile organic compound (VOC) monitoring was validated by SPME-GC-MS analysis. The system effectively tracked spoilage-related markers such as ethanol and freshness-associated volatiles including hexanal and anethole, demonstrating its potential for non-destructive quality assessment. Importantly, the authors emphasized the integration of IoT-enabled sensor platforms into commercial cold chains to enable early detection of physiological stress and quality degradation.

Complementing volatile monitoring, Wang *et al.*[72] developed a wireless multi-gas sensor system (WGS²) capable of real-time measurement of $SO_2$ (0–150 ppm, ±1 ppm accuracy), $CO_2$, $O_2$, temperature, and relative humidity during storage and transport.[72] Their findings showed that maintaining optimized $SO_2$ fumigation levels (10–20 ppm) in combination with stable low temperatures reduced quality losses to below 10%, compared with traditional losses of 25–30%. Moreover, the system enabled more accurate shelf-life prediction based on continuous atmospheric monitoring.

While these technologies significantly enhance detection capabilities, they do not inherently provide mitigation unless coupled with predictive modelling frameworks. Real-time monitoring

View Article Online
DOI: 10.1039/D6FB00142D



often remains reactive, identifying deviations after they occur rather than anticipating risk. The incorporation of sensor data streams into an integrated modelling framework, as conceptualized in Figure 7, would allow dynamic updating of boundary conditions and model parameters, enabling predictive assessment of atmospheric drift, $SO_2$ accumulation, or temperature-induced respiration shifts before physiological disorders develop.

In the context of export systems which are characterized by extended maritime transport, spatial airflow heterogeneity, and multilayer packaging with active $SO_2$ release, the value of sensor-assisted model validation is particularly high. Continuous data assimilation can improve parameter estimation for respiration kinetics, effective mass transfer coefficients, and $SO_2$ distribution models, thereby strengthening predictive accuracy under real-world variability.

Technological advancements spanning mathematical modelling, advanced packaging materials, and IoT-based smart monitoring systems are collectively reshaping postharvest management strategies for table grapes. However, the greatest impact will emerge from multidisciplinary integration rather than isolated technological adoption. Future research should therefore prioritize scalable sensor–model coupling, cost-effective deployment strategies, and cross-cultivar validation under commercial export conditions. Such integration would support more resilient cold chains, reduced quality claims, and enhanced export competitiveness. A broader overview of cold chain logistics and packaging studies is provided in Table 4. These works span airflow modelling, packaging design, shelf-life prediction, and smart monitoring, but are largely developed in isolation. This fragmentation highlights the need for integrated frameworks, where sensor data can support system-level model validation and coupling.

View Article Online
DOI: 10.1039/D6FB00142D

Table 4: Summary of key studies on cold chain logistics and packaging for table grapes

| Study | Focus Area | Key Findings | Limitations |
|---|---|---|---|
| [73] | Mathematical modelling in reefers | Model could predict mass loss during cold chain transportation | Needs real-world validation under diverse logistics scenarios |
| [69] | Biodegradable packaging films | Polysaccharide-based films retained grape quality | Cost, $SO_2$ compatibility need assessment |
| 20 | CFD modelling of airflow and moisture | Perforated liners + high humidity improved moisture retention; sidewall venting improved airflow | Needs validation across more cultivars |
| [72] | IoT-based cold chain monitoring | Real-time detection of cold chain breaches using sensors + GPS | Infrastructure-dependent |
| 5 | Shelf-life modelling | Temperature-based models predict grape shelf life | Limited data on wider range of varieties |
| [74] | Finite element modal analysis on packaging design | Identified packaging material with most effective vibrational shock suppression, proposed structural redesign | Needs broader commercial trials |
| [71] | Thermal properties of Rasa grapes | Specific heat and conductivity increased with moisture and temperature | Focused on one cultivar |
| [43] | Cooling setpoints and stacking positioning | Box stacking had an impact on the airflow pattern per stack | More varietal trials needed |

# 5 Sustainability, energy efficiency, and environmental governance in table grape cold chains

Cold chain systems for exported table grapes are multi-component and refrigeration-dependent systems with electricity consumption for temperature maintenance, maritime transport fuel use, packaging production, and product loss collectively determine greenhouse gas (GHG) emissions. In long-distance export chains, refrigeration electricity consumption and transport fuel use dominate lifecycle emissions, while packaging materials contribute through embodied carbon and end-of-life impacts.[75-77] Sustainable optimization therefore requires a systems-based perspective that integrates thermal performance, mass transfer behaviour, packaging material intensity, and lifecycle emissions, rather than isolated substitution of materials or technologies.

## 5.1 Application of carbon foot printing in table grape cold chains

View Article Online
DOI: 10.1039/D6FB00142D



Comprehensive carbon footprint analyses spanning the full table grape cold chain, from vineyard production to international distribution, remain comparatively limited in the peer-reviewed literature. However, a growing body of lifecycle assessment (LCA) and cold-chain carbon studies in fresh fruit systems provides empirical grounding for the application of carbon accounting methodologies to table grapes. Carbon foot printing in agri-food systems is typically conducted under established frameworks such as ISO 14040/14044 (LCA methodology), ISO 14067 (product carbon footprint), and the GHG Protocol (activity data × emission factor approach). These standards decompose total emissions into contributions from electricity use, fuel consumption, material production, and transport (GHG Protocol, 2011; ISO 14067, 2018). In refrigerated supply chains, electricity demand for cooling and transport emissions are consistently identified as dominant contributors.[76, 77]

Vineyard-level LCAs conducted in Mediterranean grape systems report production-stage carbon intensities broadly in the range of 0.3 to 0.9 kg $CO_2$e per kg grapes, with fertiliser production, irrigation energy, and diesel use in field operations consistently identified as the principal emission drivers.[78, 79] Notably, table grape varieties tend toward the upper end of this range owing to their more intensive agronomic inputs relative to wine grape systems.[78] Postharvest and storage-focused analyses further demonstrate the substantial contribution of refrigeration energy to the carbon footprint of fresh fruit export chains. Du Plessis *et al.*[76] assessed the energy and emission intensity of eight refrigerated cold-store facilities handling fresh fruit for export in South Africa, finding that electricity consumption was the overwhelming driver of facility-level emissions, with diesel accounting for less than 1% of total cold-store emissions. Each pallet stored requires approximately 7.62 kWh of electricity per day, translating to 7.52 kg $CO_2$e per pallet per day. Although the study was not exclusive to table grapes, the same research group explicitly included table grapes alongside oranges and apples in subsequent supply chain analyses, and the thermal storage requirements and export handling systems across these commodities are directly comparable.[76] Distribution-stage assessments of exported fresh fruits show that maritime transport emissions often range between 0.3 and 0.8 kg $CO_2$e per kg product depending on route distance, storage duration, and load efficiency (recent distribution-focused LCAs on fresh fruit export chains).[77]

View Article Online
DOI: 10.1039/D6FB00142D



Importantly, most existing studies treat lifecycle stages independently and rarely integrate carbon accounting with quality-loss modelling. Yet food loss significantly increases emissions per kilogram of marketable product because upstream emissions are allocated over a reduced saleable mass (Bhatia *et al.*[75]). In perishable commodities such as table grapes, where decay, $SO_2$ injury, or temperature abuse can lead to rejection rates exceeding 10% (postharvest loss citation), loss-adjusted carbon intensity becomes a critical but underreported metric. Improvements in airflow distribution, reduced cooling time, optimized liner permeability, and controlled $SO_2$ release, traditionally evaluated in terms of decay suppression and quality preservation, also directly influence refrigeration electricity demand and rejection rates. When emissions are expressed per kilogram of marketable fruit delivered, such improvements translate into measurable reductions in carbon intensity.

Although carbon modelling has been widely applied in fresh produce LCAs, its coupling with thermo-physiological modelling, mass transfer simulation, and digital twin frameworks remains largely unexplored. Embedding standard carbon accounting relationships within predictive cold chain simulations would enable dynamic estimation of electricity consumption, transport emissions, and loss-adjusted carbon intensity under variable commercial conditions. In this context, carbon foot printing evolves from a retrospective reporting tool into a quantitative decision-support layer within integrated cold chain optimization.

### 5.2 Sustainable packaging materials and functional trade-offs

Recent research has explored biodegradable and alternative packaging materials as strategies to reduce packaging-related environmental burdens. Silva *et al.*[80] developed a starch–glycerol–PBAT biodegradable film incorporating sodium metabisulfite sachets for $SO_2$ release in ‘Benitaka’ table grapes.[80] The system effectively suppressed mould growth over 45 days at 1°C and preserved rachis freshness, yet surface bleaching was observed. This outcome suggests that altered gas permeability and $SO_2$ retention characteristics influenced the internal atmosphere and fumigation dynamics. The study highlights that material substitution must be evaluated within respiration–diffusion–reaction frameworks rather than solely through decay suppression metrics.

Similarly, Cheng *et al.*[81] demonstrated that polyvinylidene chloride-coated white cardboard enhanced mechanical strength and reduced weight loss by approximately 5%.[81] While improved

View Article Online
DOI: 10.1039/D6FB00142D

barrier performance may reduce moisture loss, high-barrier coatings can modify internal gas exchange and humidity gradients. Without integration into predictive respiration–diffusion models, enhanced barrier properties may inadvertently shift internal $O_2$–$CO_2$ equilibrium outside cultivar-specific safety windows.

Life cycle assessment evidence indicates that although bioplastics may offer end-of-life advantages, their upstream production can remain energy-intensive.[80] Therefore, packaging sustainability must be assessed through functional performance and lifecycle trade-offs. A thicker or higher-barrier material that prolongs cooling time may increase refrigeration electricity demand, offsetting gains in embodied carbon reduction.

### 5.3 Logistics optimization and energy demand

Transport duration and thermal exposure are major determinants of cumulative respiration, refrigeration load, and product loss.[76] AI-based logistics optimization systems have demonstrated reductions in fuel consumption and improved load utilization.[82] Shorter transit times reduce cumulative heat load and respiration-driven quality degradation, indirectly lowering both transport-related and refrigeration-related emissions. Spatial thermal heterogeneity within containers, as documented in modelling and sensor-based studies, increases local respiration rates and disorder risk. By optimizing airflow distribution and reducing hotspots, refrigeration energy per unit mass can be reduced.[18] Thus, logistics optimization affects both transport-related emissions ($CF_{transport}$) and refrigeration-related emissions ($CF_{elec}$) through reductions in time–temperature exposure.

The incorporation of sustainability metrics into an integrated modelling frameworks enable dynamic carbon accounting under commercial variability. As illustrated in Figure 7, airflow modelling, liner mass transfer, and $SO_2$ release dynamics are centrally coupled through temperature-dependent respiration kinetics. Extending this framework to include energy consumption and emission factors allows real-time estimation of cumulative electricity demand, transport intensity, and predicted product loss. Under standard carbon accounting methodology, carbon intensity per functional unit is expressed as:

View Article Online
DOI: 10.1039/D6FB00142D

$CF_{intensity} = \frac{CF_{total}}{m_{saleable}}$ (16)where $CF_{\text{intensity}}$ (kg $CO_2e$ $kg^{-1}$) is the carbon intensity per unit of marketable fruit, $CF_{\text{total}}$ (kg $CO_2e$) is the total lifecycle greenhouse gas emissions associated with the system boundary considered, and $m_{\text{saleable}}$ (kg) represents the mass of marketable fruit delivered (ISO 14067; food loss GHG methodologies). This formulation highlights the sensitivity of carbon intensity to product loss, as upstream emissions are distributed over reduced saleable mass. In table grape systems, reported production-stage carbon intensities typically range between 0.4 and 0.8 kg $CO_2e$ $kg^{-1}$, while cold storage and distribution contribute an additional 7.5 kg $CO_2e$ per pallet per day and 0.3–0.8 kg $CO_2e$ $kg^{-1}$, respectively, depending on storage duration and transport distance. Product loss therefore increases emissions per kilogram of saleable fruit, as upstream cultivation, packaging, refrigeration, and transport emissions are allocated over a reduced output mass.

To provide a quantitative interpretation of the impact of cold chain duration on environmental performance, a first order estimate of carbon intensity ($CF_{\text{intensity}}$) was developed based on reported stage-wise emission factors for table grape export systems. Using a cradle-to-retail system boundary consistent with Table 5 and bottom-up aggregation of cold storage, maritime transport, and inland distribution contributions, total emissions were estimated at approximately 1.43–1.49 kg $CO_2e$ $kg^{-1}$ of product shipped. When expressed per unit of saleable fruit, this corresponds to a carbon intensity of approximately 1.58–1.71 kg $CO_2e$ $kg^{-1}$ under postharvest loss scenarios of 8–15%. These values are consistent with recent lifecycle assessments of table grape cold chains, which report carbon intensities of 1.28 kg $CO_2e$ $kg^{-1}$ for shorter supply chains, increasing to approximately 1.63 kg $CO_2e$ $kg^{-1}$ with an additional month of cold storage. This relationship can be approximated by a linear model:

$$CF_{\text{intensity}}(t) = 1.28 + 0.0117\,t \quad (17)$$

where $t$ is storage duration in days. As shown in Figure 8, this implies that carbon intensity increases by approximately 0.35 kg $CO_2e$ $kg^{-1}$ over a 30-day storage period, highlighting cold chain duration as a first-order driver of emissions. Importantly, this increase is further amplified by product loss, as emissions are attributed to the reduced mass of saleable fruit. As a result, the

View Article Online
DOI: 10.1039/D6FB00142D

combined effect of extended storage (e.g., ~30 days) and moderate losses can elevate carbon intensity to values approaching 1.6–1.7 kg $CO_2$e $kg^{-1}$, effectively exceeding the mass of the product itself on a carbon-equivalent basis. This illustrates the strong coupling between postharvest quality management and environmental performance and reinforces the need for integrated strategies that simultaneously optimize storage duration, packaging design, and loss mitigation.

Table 5: Parameters and values used for estimating carbon intensity of table grape supply chains (vineyard to retail)

| Parameter | Value | Basis |
|---|---|---|
| System boundary | Vineyard → retail shelf (cradle-to-distribution) | Consistent with LCA system definitions[76, 77] |
| Production stage | | |
| Farm-level emissions | 0.51 kg $CO_2$e $kg^{-1}$ | Reported LCA value[78] |
| Packhouse emissions | 0.15 kg $CO_2$e $kg^{-1}$ | Postharvest handling emissions[76] |
| Production subtotal | ~0.66 kg $CO_2$e $kg^{-1}$ | Aggregated |
| Distribution stage | | |
| Cold storage emission factor | 7.52 kg $CO_2$e $pallet^{-1}$ $day^{-1}$ | Measured cold storage emissions[76] |
| Storage duration | 30 days | Extended cold chain scenario[76] |
| Pallet load | ~1,080 kg | Typical commercial configuration |
| Storage emission (per kg) | 0.209 kg $CO_2$e $kg^{-1}$ | Derived |
| Maritime transport | 0.52 kg $CO_2$e $kg^{-1}$ | Derived to match transport contribution[77] |
| Last-mile distribution | 0.05–0.10 kg $CO_2$e $kg^{-1}$ | Consistent with LCA distribution breakdown[77] |
| Distribution subtotal | ~0.77–0.83 kg $CO_2$e $kg^{-1}$ | Aggregated |
| Total (cradle-to-retail) | ~1.43–1.49 kg $CO_2$e $kg^{-1}$ | Bottom-up integrated estimate |

View Article Online
DOI: 10.1039/D6FB00142D



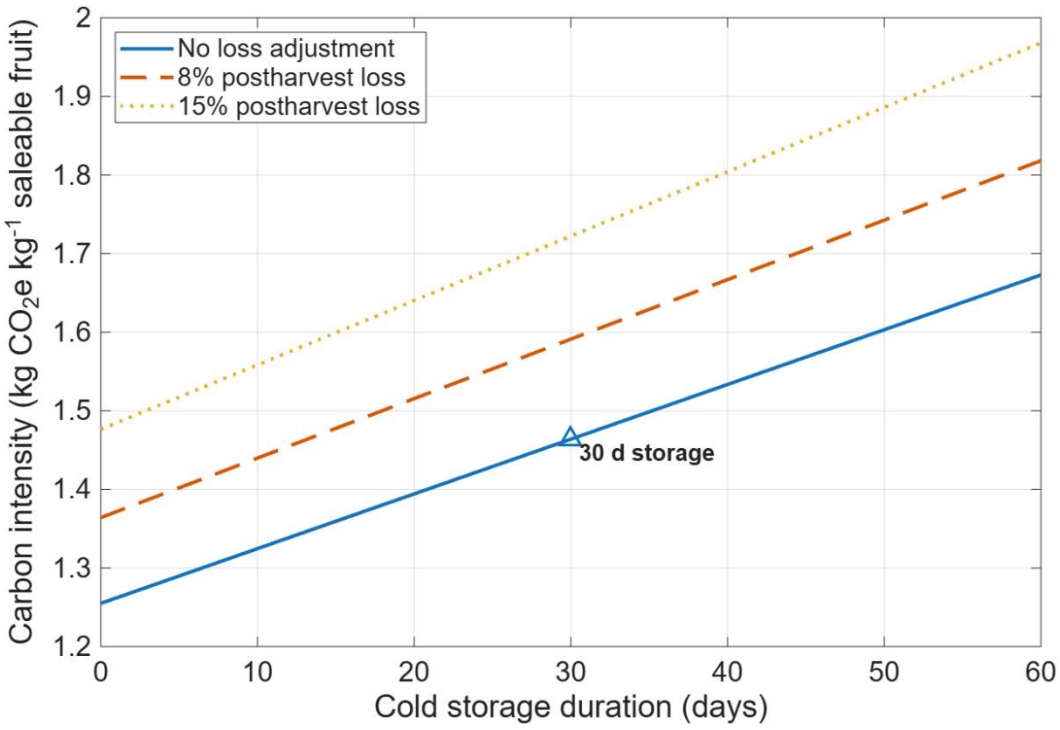


Figure 8: Predicted carbon intensity ($CF_{intensity}$) of table grapes as a function of cold storage duration under export conditions. The relationship is approximated using a linear model derived from reported lifecycle assessments, showing an increase of ~0.35 kg $CO_2$e kg$^{-1}$ over 30 days of storage.

### 5.4 Policy and regulatory drivers

Environmental governance frameworks increasingly require quantifiable reductions in emissions intensity and packaging waste. Standards such as GlobalG.A.P., GRASP, and the Sustainability Initiative of South Africa (SIZA) incorporate environmental performance metrics, while the European Green Deal and Farm to Fork Strategy mandate reductions in packaging waste and lifecycle emissions for exported produce. These drivers shift sustainability from voluntary practice to measurable performance. Integration of lifecycle assessment and carbon accounting within predictive cold chain models enables exporters to quantify emissions intensity per kilogram of delivered fruit under real operating conditions. In this context, the carbon intensity formulation (Eqn. 16), together with the parameterization in Table 5 and the storage–loss relationship illustrated in Figure 8, provides a practical basis for linking operational decisions to environmental performance. Integrated modelling framework architectures capable of estimating energy demand, carbon intensity, and loss-adjusted output enable scenario-based evaluation and support evidence-based environmental reporting.

View Article Online
DOI: 10.1039/D6FB00142D



Sustainability in table grape cold chains cannot be achieved through isolated improvements in packaging material or energy efficiency. Refrigeration load, packaging geometry, liner permeability, $SO_2$ fumigation dynamics, transport duration, and product loss are thermally and kinetically coupled processes. Embedding carbon accounting relationships, consistent with GHG Protocol and ISO methodologies, within the integrated modelling framework (Figure 7) transforms sustainability from a descriptive objective into a predictive, systems-level optimization problem. By linking respiration kinetics, airflow distribution, liner mass transfer, $SO_2$ release, and lifecycle carbon metrics, cold chain management can transition from reactive mitigation toward performance-based environmental optimization under commercial variability.

# 6 Conclusion and Future Directions

This review demonstrates that the postharvest performance of table grapes is governed by tightly coupled interactions between temperature, relative humidity, packaging architecture, and $SO_2$-mediated decay control, rather than by any single factor. Evidence reviewed here shows that widely adopted uniform cold chain prescriptions fail to account for the heterogeneous microenvironments created within modern multi-layer packaging systems. As a result, fruit quality outcomes are often dictated by within-package and within-pallet variability rather than nominal storage set-points.

A central insight emerging from this review is that trade-offs are unavoidable: conditions that minimize rachis dehydration (high RH, restricted ventilation) frequently exacerbate decay and $SO_2$-related injury, while strategies that enhance cooling and gas exchange can intensify moisture loss and quality heterogeneity. These competing responses are further modulated by cultivar-specific physiology and storage duration, underscoring the limitations of generalized handling protocols.

Future progress depends on transitioning from empirical guidelines to mechanistically informed, configuration-specific control strategies. This requires (i) explicit integration of heat, mass, and gas transport processes with fruit physiological responses; (ii) quantification of spatial variability within commercial packaging systems; and (iii) alignment of $SO_2$ release dynamics and emerging technologies such as 1-MCP with the actual microclimates experienced by the fruit. In parallel,

View Article Online
DOI: 10.1039/D6FB00142D

the adoption of sensor-enabled monitoring and predictive analytics offers a pathway toward real-time optimization of cold chain performance.

Advancing the table grape industry will therefore depend on treating packaging and cold chain operations as a coupled, multiphase system, where design and control are guided by quantitative understanding rather than convention. Such a shift is essential to simultaneously achieve quality preservation, regulatory compliance, and operational efficiency in increasingly demanding export markets.

## 7 Acknowledgements

This work was supported by the National Research Foundation (NRF) (Grant No. **CPRR240316209462**). Buhle Maphosa is a postdoctoral fellow funded by the National Research Foundation (NRF).

## 8 Conflict of interest statement

The authors declare no conflict of interest.

## 9 References

1. T. Ejsmentewicz, I. Balic, D. Sanhueza, R. Barria, C. Meneses, A. Orellana, H. Prieto, B. G. Defilippi and R. Campos-Vargas, Molecules, 2015, 20, 3667–3680.

2. N. Hamie, J. P. Zoffoli, L. Tarricone, V. Verrastro, A. G. Pérez-Donoso and G. Gambacorta, Postharvest Biology and Technology, 2022, 184, 111758.

3. U. Khalil, I. A. Rajwana, K. Razzaq, U. Farooq, B. A. Saleem and J. K. Brecht, South African Journal of Botany, 2023, 154, 273–281.

4. A. Blanckenberg, U. L. Opara and O. A. Fawole, Sustainability, 2021, 13, 4450.

5. S. Fedeli, L. Goedhals-Gerber and E. van Dyk, Transportation Research Procedia, 2022, 67, 63–71.

6. A. Ambaw, M. Mukama, T. Fadiji and U. L. Opara, Food Packaging and Shelf Life, 2021, 32, 100858.

7. A. Ambaw, M. Mukama, T. Fadiji and U. L. Opara, 2022, https://doi.org/10.17660/ActaHortic.2022.1349.53, 389–398.

View Article Online
DOI: 10.1039/D6FB00142D



8. T. M. Berry, T. Defraeye, A. Ambaw, C. J. Coetzee and U. L. Opara, Biosystems Engineering, 2022, 220, 181–202.

9. M. Ngcobo, U. Opara and G. Thiart, Packaging Technology and Science, 2012, 25, 73–84.

10. J. Pinto, M. Schorr, F. Thewes, D. Ceconi, V. Both, A. Brackmann and D. Fronza, Ciência Rural, 2015, 45, 386–391.

11. R. Lufu, A. Ambaw, T. M. Berry and U. L. Opara, Food Packaging and Shelf Life, 2020, 26, 100585.

12. R. Lufu, A. Ambaw and U. L. Opara, Postharvest Biology and Technology, 2019, 157, 110982.

13. S. Ahmed, S. R. Roberto, A. R. Domingues, M. Shahab, O. J. C. Junior, C. H. Sumida and R. T. De Souza, Horticulturae, 2018, 4, 29.

14. A. C. de Aguiar, M. T. Higuchi, F. Yamashita and S. R. Roberto, Horticulturae, 2023, 9, 724.

15. O. J. C. Junior, K. Youssef, R. Koyama, S. Ahmed, A. R. Dominguez, D. T. Mühlbeier and S. R. Roberto, Pathogens, 2019, 8, 271.

16. B. C. Dantas, M. T. Higuchi, A. C. de Aguiar, B. E. Bosso and S. R. Roberto, Horticulturae, 2022, 8, 285.

17. A. Lichter, T. Kaplunov, Y. Zutahy and S. Lurie, Israel Journal of Plant Sciences, 2016, 63, 2–6.

18. A. Ambaw, P. Verboven, T. Defraeye, E. Tijskens, A. Schenk, U. L. Opara and B. M. Nicolai, Journal of Food Engineering, 2013, 119, 150–158.

19. A. Ambaw, P. Verboven, M. A. Delele, T. Defraeye, E. Tijskens, A. Schenk, B. E. Verlinden, U. L. Opara and B. M. Nicolai, Food and Bioprocess Technology, 2014, 7, 1903–1916.

20. M. A. Delele, B. Vorstermans, P. Creemers, A. A. Tsige, E. Tijskens, A. Schenk, U. L. Opara, B. M. Nicolaï and P. Verboven, Journal of Food Engineering, 2012, 108, 59–68.

21. A. Owoyemi, M. Balaklav, B. Kochanek, R. Porat, N. Koenigstein, Y. Salzer and A. Lichter, Postharvest Biology and Technology, 2024, 215, 113013.

22. Z. Wu, X. Yuan, H. Li, F. Liu, Y. Wang, J. Li, H. Cai and Y. Wang, Postharvest Biology and Technology, 2015, 105, 26–33.

View Article Online
DOI: 10.1039/D6FB00142D

23. E. Poeta, M. L. V. de Chiara, M. Cefola, I. Caruso, D. Genzardi, E. Núñez-Carmona, B. Pace, M. Palumbo and V. Sberveglieri, Postharvest Biology and Technology, 2025, 227, 113587.

24. X. Xiao, Q. He, Z. Li, A. O. Antoce and X. Zhang, Food Control, 2017, 73, 1556–1563.

25. X. Xiao, X. Wang, X. Zhang, E. Chen and J. Li, Applied Sciences, 2015, 5, 747–760.

26. V. Alba, A. Russi, G. Forte, R. A. Milella, S. Roccotelli, P. Campi, A. F. Modugno, V. Pipoli, G. Gentilesco, L. Tarricone and A. R. Caputo, Sustainability, 2024, 16, 3543.

27. A. Lichter, T. Kaplunov, Y. Zutahy, A. Daus, V. Alchanatis, V. Ostrovsky and S. Lurie, Postharvest Biology and Technology, 2011, 59, 25–33.

28. S. Tao, J. Wang and J. Xie, Food Quality and Safety, 2024, 8.

29. L. Ruiz-Garcia, P. Barreiro, A. Anand and J. I. Robla, 2008, https://doi.org/10.17660/ActaHortic.2008.802.51, 385–390.

30. M. T. Talbot and C. D. Baird, 1992.

31. A. Lichter, Australian Journal of Grape and Wine Research, 2016, 22, n/a–n/a.

32. Y. Zhang and M. Keller, American Journal of Enology and Viticulture, 2015, 66, 454–462.

33. M. Amorim, B. Miranda, I. Santos, S. Turco, B. Caçula, D. Lourençoni and G. M, Agrária - Revista Brasileira de Ciências Agrárias, 2021, 15, 1–8.

34. Á. Navarro-Calderón, N. Falagán, L. A. Terry and M. C. Alamar, Frontiers in Plant Science, 2023, Volume 14 - 2023.

35. M. Ngcobo, Masters, Stellenbosch University, 2008.

36. L. Li, T. Kaplunov, Y. Zutahy, A. Daus, R. Porat and A. Lichter, Postharvest Biology and Technology, 2015, 107, 16–22.

37. R. Rosales, C. Fernandez-Caballero, I. Romero, M. I. Escribano, C. Merodio and M. T. Sanchez-Ballesta, Postharvest Biology and Technology, 2013, 77, 50–58.

38. N. Dimopoulos, R. Tindjau, D. C. J. Wong, T. Matzat, T. Haslam, C. Song, G. A. Gambetta, L. Kunst and S. D. Castellarin, Journal of Experimental Botany, 2020, 71, 3126–3141.

39. A. Lichter, Y. Zutahy, T. Kaplunov and S. Lurie, HortTechnology, 2008, 18, 206–214.

View Article Online
DOI: 10.1039/D6FB00142D

40. I. Balic, A. Moreno, D. Sanhueza, C. Huerta, A. Orellana, B. G. Defilippi and R. Campos-Vargas, Postharvest Biology and Technology, 2012, 72, 47–56.

41. SATI, Key Concepts in Post-harvest Management of grapes, SATGI, South Africa, 2015.

42. M. Mukama, A. A. Tsige, R. Lufu and U. L. Opara, Food Packaging and Shelf Life, 2024, 46, 101380.

43. M. E. K. Ngcobo, M. A. Delele, U. L. Opara and C. J. Meyer, Journal of Food Engineering, 2013, 116, 613–621.

44. J. L. Henríquez and S. Pinochet, 2016, https://doi.org/10.17660/ActaHortic.2016.1144.39, 267–272.

45. S. C. Fonseca, F. A. R. Oliveira, I. B. M. Lino, J. K. Brecht and K. V. Chau, Journal of Food Engineering, 2000, 43, 9–15.

46. E. Raban, T. Kaplunov, Y. Zutahy, A. Daus, V. Alchanatis, V. Ostrovsky, S. Lurie and A. Lichter, Postharvest Biology and Technology, 2013, 84, 88–95.

47. S. Chen, H. Wang, Q.-q. Fu, R.-r. Wang, W. Zhang and X.-q. Cai, Packaging Technology and Science, 2018, 31, 491 – 497.

48. A. C. de Aguiar, B. E. B. Caetano and S. R. Roberto, Horticulturae, 2024, 10, 924.

49. Z. Li, J. Huang, H. Chen, M. Yang, D. Li, Y. Xu, L. Li, J. Chen, B. Wu and Z. Luo, Food Chemistry, 2023, 408, 135188.

50. M. T. Higuchi, A. C. d. Aguiar, N. R. Leles, L. T. M. Ribeiro, B. E. C. Bosso, F. Yamashita, K. Youssef and S. R. Roberto, Horticulturae, 2024, 10, 214.

51. J.-S. Lee, T. Kaplunov, Y. Zutahy, A. Daus, N. Alkan and A. Lichter, Scientia Horticulturae, 2015, 192, 346–349.

52. X. Y. Jia, X.-l. Hao, Y. Zheng, J. Zhang, Y. Li, X. Li and Z. Zhao, Journal of Food Processing and Preservation, 2020, 44.

53. X. Chen, Z. Zhu, Z. Xiaoshuan, O. Antoce and W. Mu, Journal of Food Processing and Preservation, 2016, 41.

54. A. R. Domingues, S. R. Roberto, S. Ahmed, M. Shahab, O. José Chaves Junior, C. H. Sumida and R. T. De Souza, Horticulturae, 2018, 4, 17.

55. K. Youssef, S. R. Roberto, F. Chiarotti, R. Koyama, I. Hussain and R. T. de Souza, Scientia Horticulturae, 2015, 193, 316–321.

View Article Online
DOI: 10.1039/D6FB00142D

56. T. Kaplunov, Y. Zutahy, S. Lurie and A. Lichter, Quality Assurance and Safety of Crops & Foods, 2011, 3, 191–197.

57. Y. Yuan, J. Wei, S. Xing, Z. Zhang, B. Wu and J. Guan, Postharvest Biology and Technology, 2022, 190, 111953.

58. H. N. Abdelhamid and A. P. Mathew, Frontiers in Chemical Engineering, 2021, Volume 3 - 2021.

59. R.-J. Shi, T. Wang, J.-Q. Lang, N. Zhou and M.-G. Ma, Frontiers in Bioengineering and Biotechnology, 2022, Volume 10 - 2022.

60. M. I. Elsayed, A. D. Al-Qurashi, N. M. Almasaudi and K. A. M. Abo-Elyousr, South African Journal of Botany, 2022, 146, 481–490.

61. S. Luesuwan, M. Naradisorn, K. A. Shiekh, P. Rachtanapun and W. Tongdeesoontorn, Polymers, 2021, 13, 3445.

62. S. T. Olorunsogbon, M. ÖZden and I. T. Riley, Applied Ecology and Environmental Research, 2023, 21, 3533–3559.

63. X. Yun, L. Zhang, T. Dong, H. Zhang, T. Sun, J. Hu and P. Cheng, Food Sci Nutr, 2025, 13, e71176.

64. F. J. Soldateli, V. Both, C. B. Batista, M. R. Pasquetti Berghetti, V. Ludwig, L. M. Wendt, A. Brackmann and F. R. Thewes, Applied Fruit Science, 2025, 67, 36.

65. S. Eshghi, R. Karimi, A. Shiri, M. Karami and M. Moradi, Journal of Food Measurement and Characterization, 2021, 15, 3683–3693.

66. C. Melo, N. Ferrão, B. L. de MendonçaSoares, K. Marques Diniz, C. Ferreira Leal, D. Canto, M. A. P. Flores, J. Henrique da Costa Tavares-Filho, A. Galembeck, T. L. Montenegro Stamford, T. Montenegro Stamford-Arnaud and T. C. Montenegro Stamford, Postharvest Biology and Technology, 2018, 139, 56–66.

67. H. Cui, M. Abdel-Samie and L. Lin, Journal of Food Process Engineering, 2019, 42.

68. M. Cefola and B. Pace, European Journal of Horticultural Science, 2016, https://doi.org/10.17660/eJHS.2016/81.4.2197–203.

69. M. P. Indumathi, K. Saral Sarojini and G. R. Rajarajeswari, International Journal of Biological Macromolecules, 2019, 132, 1112–1120.

70. T. Fadiji, A. Ambaw, C. J. Coetzee, T. M. Berry and U. L. Opara, Biosystems Engineering, 2018, 174, 260–281.

View Article Online
DOI: 10.1039/D6FB00142D

71. H. Akhijahani and J. Khodaei, World Applied Sciences Journal, 2013, 22, 939–947.

72. X. Wang, Q. He, M. Matetic, T. Jemric and X. Zhang, Computers and Electronics in Agriculture, 2017, 135, 195–207.

73. E. Pereira, R. Gonçalves Broco e Silva, W. Spagnol and V. Junior, Food Science and Technology (Campinas), 2017, 38.

74. M. Yin, L. Huo, N. Li, H. Zhu, Z. Zhu and J. Hu, Food Control, 2024, 165, 110684.

75. P. C. Bhatia, C; Draucker, L.; Rich, D; Lahd, H; ; Brown, A, 2011, 148.

76. M. du Plessis, J. van Eeden and L. L. Goedhals-Gerber, Heliyon, 2024, 10, e32507.

77. M. du Plessis, J. van Eeden and L. L. Goedhals-Gerber, Transportation Research Interdisciplinary Perspectives, 2025, 32, 101551.

78. V. D. Litskas, T. Irakleous, N. Tzortzakis and M. C. Stavrinides, Journal of Cleaner Production, 2017, 156, 418–425.

79. I. Vázquez-Rowe, P. Villanueva-Rey, M. T. Moreira and G. Feijoo, Journal of Environmental Management, 2012, 98, 73–83.

80. R. J. Silva, A. C. de Aguiar, B. M. Simões, S. C. da Silva, M. T. Higuchi, S. R. Roberto and F. Yamashita, Polymers, 2024, 16, 274.

81. Z. Cheng, J. Li, M. Su, N. Xiao, L. Zhong, X. Zhang, M. Liu, Q. Chen and J. Zhou, RSC Advances, 2024, 14, 20479–20491.

82. S. Nguyen, X. Fu, L. Zhao, H. Xu, X. Zhang, N. Li, W. Zhang, X. F. Yin, O. Daichi, J. Koh and Q. Zheng, Transportation Research Part E: Logistics and Transportation Review, 2026, 207, 104569.

83. W. Carina, Confronting Climate Change Benchmark Report, Blue North Sustainability, South Africa, 2022, Blue North Sustainability.



View Article Online
DOI: 10.1039/D6FB00142D

## Data Availability Statements

Data sharing is not applicable to this article as no new data were created or analysed in this study.